Inelastic processes in 1-1000 keV/u collisions of Be^{q+} (q=2-4) ions with atomic and molecular hydrogen

D.R. Schultz, P.S. Krstić, and C.O. Reinhold

Controlled Fusion Atomic Data Center and Physics Division, Oak Ridge National Laboratory, Oak Ridge, Tennessee 37831-6373, USA

Abstract

Owing to the use of beryllium in fusion reactors and the consequent need to model and diagnose plasmas containing this species of impurity, cross sections are presented here for inelastic collisions of 1-1000 keV/u Be^{q+} (q=2-4) with H and H_2. In particular, the classical trajectory Monte Carlo technique is used to compute total cross sections for (*i*) ionization, (*ii*) state-selective excitation, and (*iii*) state-selective charge transfer.

1 Introduction

Beryllium is among the proposed plasma facing materials in next-step fusion reactors such as the *International Thermonuclear Experimental Reactor*, and is a species already used in some present fusion devices. Its utility derives from the unique combination of thermo-physical properties and low atomic number that it possesses. The materials which form the first surface with which the plasma may come into contact will chemically and physically sputter impurities which may enter the central plasma and have a deleterious effect on maintaining the conditions required for a burning plasma. Since the undesired radiation losses generated by plasma impurities grows strongly with the atomic number, Z, of the ion, a low-Z material is potentially advantageous. Present designs seek to replace certain first surface materials such as Ni, Fe, or Mo, with low-Z materials such as C, boronated carbon fibers, or beryllium. Thus, the interest in beryllium (Z=4) since it is also a suitably strong and resilient metal. Furthermore, it is hoped that atomic and molecular processes in the edge-plasma layer will suppress impurity ingress (see e.g. [1]).

Consequently, it is important to have a knowledge of the various inelastic cross sections for interaction of beryllium ions with the principal plasma components. Excitation, ionization, and charge transfer cross sections can be used as input to plasma models seeking to describe, for example, the charge state balance and impurity transport properties of edge plasmas. In addition, state-selective charge transfer cross sections may be employed to diagnose plasma properties such as its rotation through charge exchange recombination spectroscopy.

Therefore, since tabulations have not appeared providing coverage of these cross sections over a significant range of collision energy and charge states, we employ here a relatively simple and reliable method, the classical trajectory Monte Carlo (CTMC) technique, to compute cross sections for ionization and state-selective excitation and charge transfer. A large body of work has shown that the CTMC method provides a reasonable and accurate estimate of these cross sections for intermediate collision velocities for bare ions colliding with H, H_2, and He. Some results have also been obtained for partially stripped impinging ions with reasonable agreement found with experiments, but with less overall certainty, since a full treatment would have to include the multielectronic transitions possible in such a case. Since theoretical methods with which a large range of ionic charges and collision energies could be covered more robustly is not readily available, the CTMC results provide a first estimate of the required processes.

That is, the complete quantum mechanical treatment of an arbitrary ion, carrying possibly several electrons, colliding with atomic or molecular hydrogen, is a difficult, multi-electron, many-state calculation. The CTMC technique, in its one-active-electron, many-active-electron, or model-potential formulations serves as a very useful tool to produce a broad range of required data. Careful comparison with other more robust methods for a set of fundamental channels allows one to assess the range of reliability of the CTMC results, and to extend with some reasonable level of confidence to other similar systems. Previous works have, for example, tabulated state selective charge transfer cross sections for C^{6+} and O^{8+} with atomic hydrogen [2] and He^{2+} with H in both the ground and n=2 states of hydrogen [3], and total electron loss cross sections for Fe ions colliding with H, H_2, and He [3].

Here we compute cross sections concerning excitation, ionization, and charge transfer for fully stripped beryllium ions colliding with atomic hydrogen, and compare them with results of close coupling calculations and the theory of hidden crossings which are tractable for this one-electron system. Then, since such fully quantum calculations are not feasible for multielecton collision systems for the required range of reaction channels, we provide CTMC results for $Be^{2,3+}$ + H, and for $Be^{2,3,4+}$ + H_2.

The basic CTMC method has been described by Abrines and Percival [4] and Olson and Salop [5], and particular applications pertinent to computing excitation by Reinhold, Olson, and Fritsch [6], state-selective capture by Becker and MacKellar [7] (see also Refs. [2, 3]), collisions involving modeling H_2 by Meng, Reinhold, and Olson [8], and for collisions in which the inactive projectile electrons are represented by a model potential by Peach *et al.* [9] and Toburen *et al.* [10], for example. We proceed here by assessing the range of applicability of the CTMC results for each system where there are other data for comparison, and then present the results over this range for all of the ions and targets considered.

2 Ionization

In Figure 1 we compare the present CTMC result for ionization of atomic hydrogen by Be^{4+} impact, compared with the result from the theory of hidden crossings [11]. It has generally been found that below the maximum of the cross section the hidden crossing (HC) technique is accurate, and that around the maximum CTMC is within its limits of validity. Thus, a smooth curve joining the HC and CTMC curves usually gives a reasonable recommended cross section extending from low to intermediate energies. In this case, the CTMC method appears to be applicable above about say, 50-80 keV/u. The CTMC result for lower charges states of the beryllium ion are shown in Figure 2 compared to that for Be^{4+}. At high energy the ordering of the cross sections is according to the ionic charge state, q, in rough agreement with the q^2 scaling of the cross section predicted by first order perturbation theory (the Born approximation). At lower energies the increased charge transfer cross section for the higher charge states reduces the flux going to ionization, and the ordering of the ionization cross sections is reversed. We display the CTMC results extending to low energies to illustrate this trend, and since for the lower charge states, the limit of validity is expected to move to lower energy.

In Figures 3, 4 and 5 we display the ionization cross section for Be^{4+}, Be^{3+}, and Be^{2+}, respectively, colliding with molecular hydrogen. In this case, the ionization cross section is actually the sum of several individual contributions: single ionization (including both dissociative and non-dissociative ionization), double ionization, and transfer ionization (including Auger electron emission following double capture). The sum of these cross sections, weighted by the number of electrons liberated in each case, is usually termed the free electron production cross section. Below about 20-50 keV/u, transfer ionization is the primary component of the free electron production since charge transfer is dominant. Above this energy, capture quickly drops off and direct, single ionization dominates the sum. Since the CTMC charge transfer cross section is applicable to rather low energies due to the quasi-resonance of electron capture in these systems, and since transfer ionization dominates the "ionization" cross section at low energies, the result for free electron production is probably reasonable down to lowest energies displayed. Below 5 to 10 keV, Meng *et al.* [8] found that the available experiments for multiply charged ion impact of H_2 seemed to decrease at whereas the CTMC result plateaued. They concluded that the CTMC model for autoionization was therefore possibly inadequate, and so we report the cross section only down to this energy range, below which is may begin to drop.

3 Excitation

For Be^{4+} + H, independent theoretical data also exists for excitation to H(n=2) and H(n=3). These are displayed along with the present CTMC result in Figure 6. For n=2, the hidden crossings result [11] supports the CTMC calculation down to about 20 keV/u, while the atomic orbital (AO) close coupling result of Fritsch [12] indicates that CTMC might be reasonable to even lower energies for this state. Surprizingly the other AO calculation of Fritsch (quoted in Ref. [11]) is uniformly about a factor of two smaller. For n=3, the AO calculation is about twice as large as the CTMC result throughout the energy range of 5-100 keV/u. Evidently, CTMC and the AO theory both display an undulations in the cross section as a function of energy in the same locations, while HC does not show this behavior. Fritsch has explained this structure as being due to a type of resonance [13].

The CTMC results for Be^{4+}, Be^{3+}, and Be^{2+} colliding with H are given in Figures

7, 8, and 9, and show the cross section for excitation to the 2s, 2p, 3s, 3p, 3d, and n=2-8 states of H.

For H_2 targets, computation of detailed ro-vibronic excitation by beryllium ions would be a difficult task, given the constraints of the present survey. In addition, electronic excitation of H_2 leads to dissociative channels. Thus, to model the dissociative channels, we have taken a simpler approach. To estimate the cross section for dissiociation (i.e. for $Be^{q+} + H_2 \rightarrow H + H + Be^{q+}$) we have simply monitored the change of total binding energy for each ion trajectory in our CTMC simulation for which both electrons remain bound. If the change in electronic energy is less than the experimental dissociation threshold (4.75 eV) then the molecule is assumed to have stayed in either its ground state or some non-dissociative ro-vibronic state. If the energy change is between 4.75 eV and this value plus the first ionization potential of H (i.e. the dissociative-ionization threshold) then it is assumed that dissociation has taken place. The result of this calculation is given in Figure 10.

In addition, we can estimate the dissociative ionization and charge transfer cross sections. Shah and Gilbody [14] have measured both the dissociative and non-dissociative ionization cross sections for a range of projectiles similar in ionic and nuclear charge to those considered here (e.g. H^+, He^{2+}, $Li^{1,2,3+}$, and $C^{2,3,4+} + H_2$). From these measured cross sections we have computed the ratio of dissociative to non-dissociative ionization and found that a functional form can easily be determined which fits the ratio as a function of q, Z and impact energy. Using this fitted form of the ratio, we have multiplied the CTMC result for single ionization of H_2 by the appropriate factor to estimate that portion which should be dissociative. This estimate is also displayed in Figure 10. Regarding dissociative capture, since no estimate of the branching ratio between dissociative and non-dissociative capture exists that we are aware of, we analogously use the ratio derived for ionization to estimate the dissociative fraction of the single charge transfer result. The effect of this branching ratio is that at low energies the dissociative channel takes most of the flux, with the non-dissociative processing increasing in magnitude with increasing energy. The range of the effect of including the branching ratio is no more than an order of magnitude modification of the single ionization (or charge transfer) cross section either up or down.

As Figure 10 illustrates, at low energies the capture channel which is dominant leads to the dominance of the dissociative capture process. Ionization, which peaks at intermediate energies, is responsible for the peak of dissociative ionization at around 100 keV/u. Since both dissociative ionization and charge transfer lead to the production of H and H^+ in the final state, their sum would be a rather flat result between 1 and 1000 keV/u. Similarly, the dissociation process seems to have a rather slow dependence on impact energy in this range, sloping upward gradually in contrast to the sum of dissociative ionization and charge transfer which slowly decreases with energy. We find that the impact parameter dependence of the dissociation process has a more or less constant range, peaks at about half this maximum impact parameter, vanishing at either extreme, and that with increasing energy the magnitude of the probability simply increases. This is in contrast with the behavior of the capture or ionization probabilities which have widely varying ranges as a function of impact energy. This behavior for dissociation would indicate that regardless of the impact energy there is a reasonable likelihood of transferring the small amount of energy needed to produce dissociation. At small impact parameters it is more likely that a significant perturbation occurs and other channels are more important. Since to our knowledge, there are no calculations or measurements of these cross sections for beryllium or any similar ions, it is difficult to assess the relative accuracy of our estimates, but they should serve as a first approximation.

4 Charge Transfer

The present CTMC result for charge transfer in Be^{4+} + H is compared in Figure 11 with those from HC [11], AO [12], and molecular orbital (MO) [15] calculations. Also shown is the recommended cross section given by Janev *et al.* [16]. The consensus would indicate that below 100 keV, the CTMC result may be about fifty percent too low, but the good agreement with the AO calculation is evidence that for higher energies the fall off is well represented. The recommended curve seems to somewhat overshoot the maximum. At low energies the cross section should drop as indicated by the MO and HC results. CTMC plateaus at low energy due to the fact that it essentially gives an over-the-barrier like result for capture into non-quantized energy levels. Thus, over the energy range described here, the CTMC result should be good to within about fifty percent.

Other theories also exist for charge transfer in $Be^{2,3+}$ + H and are compared with the CTMC result in Figure 12. The perturbed stationary state (PSS) calculation of Wetmore *et al.* [17] and the Landau-Zener result of Bates and Moiseiwitsch [18] similarly show that CTMC may be about a factor of two too small in the range 1 to 20 keV/u, and that the cross section should drop off at lower energies. However, the drop off seems to be more gradual than that in the Be^{4+} case. For Be^{3+}, the MO calculations of Shimakura [19] reach the CTMC calculations by about 10 keV, but drop off more rapidly at lower energies. These observations, along with the general range of validity of the CTMC method, lead to the conclusion that the charge transfer cross section should be reasonable estimated between about 10 and 200 keV/u.

For comparison among the results for the various ions, the charge transfer cross section computed using the CTMC method is shown in Figure 13 for $Be^{2,3,4+}$ + H. The drop in going from Be^{3+} to Be^{2+} is larger than that in going from Be^{4+} to Be^{3+} since the innermost shell has been closed at the same time that the propensity of the capture cross section has shift to the lowest n-level. The degree to which the CTMC n distribution agrees with other theories is shown in Figure 14 for Be^{4+}. As has been found by a number of studies previously (see e.g. Ref. [20, 2]) the captured electron preferentially preserves both its original energy and orbital dimensions leading to the fact that it predominantly ends up with final principal quantum number $n \sim q^{3/4}$. Thus, for Be^{4+} capture to n=3 is the dominant channel, with capture to n=4 and 2 next in magnitude. As indicated by Figure 14, there is very good agreement between the AO, HC, and CTMC results for n=3. For n=4 AO and CTMC agree about 50 keV/u, and HC and AO agree fairly well below 20 keV/u. For the higher n-levels, the is rough agreement between CTMC and AO at low energies, even accounting for the undulation in the cross section (similar in origin to that discussed above for excitation), and much better agreement for higher energies.

Given these considerations, we have presented the state-selective (i.e. n, ℓ resolved) charge transfer cross sections for $Be^{2,3,4+}$ + H between 10 and 200 keV/u, where the model appears to give reasonable estimates. These are tabulated explicitly in Tables 1 to 15, and n resolved cross sections up to $n = 10$ are depicted in Figures 15 to 17. Since we represent the interaction of the electron in hydrogen with the projectile only through a model potential for $Be^{2,3+}$, we note that capture proceeds to the n=1 level when quantum mechanically it should not. In fact, due to the propensity for capture to lower n-levels for lower charge state projectiles, this deficiency is exacerbated for these ions. However, for Be^{3+}, since there is an n=1 vacancy, this should not create too great a problem. At most, the CTMC results should be decreased by a factor of two allowing for the statistical spin composition of an impacting beam of projectiles. Concerning capture by Be^{2+} since the n=1 shell is closed, we have assumed that capture can not take place to this level. The lack of a feasible way to remedy this capture into shells which are in actuality closed in this model has lead us to display calculations for only those ions where this unphysical process is not too large. For example, calculations with this model for Be^{+} lead to a very large amount of capture to n=1. The extent to which this deficiency affects the cross sections for the higher n-levels has not systematically been studied, partly for lack of extensive experimental measurements for comparison.

For molecular hydrogen targets, we utilized the model of Meng *et al.* except that we have chosen a more realistic procedure to handle autoionization after double capture. In the Meng *et al* model, the Auger electron was emitted with zero energy and all the electronic energy in the doubly excited state was left over to determine the bound n-level after emission and the l-level was always assumed to be zero. Here we assume that the electron which is in the higher n state will be emitted, carrying off energy commensurate with the total electronic energy, while the other electron will drop one level, preserving its angular momentum. Inclusion of an autoionization model is quite important, since as we have seen above, transfer ionization is the dominant process at low energies leading to final states containing a captured electron.

In Figure 18, we compare the present CTMC results for single capture for $Be^{2,3,4+}$ + H_2 with the combined AO-MO calculations of Kimura [21]. For the fully stripped ion, the CTMC results at low energies are about fifty percent smaller than the AO-MO cross sections, while for the partially stripped ions, they are a little larger in comparison. Considering the difficulty of the many electron calculation, the agreement is acceptably good.

Similar to the case of ionization, for multielectonic targets there are several processes which can lead to the capture of a single electron. In this case they are single capture or transfer ionization. The sum of these two is usually referred to simply as "$\sigma_{q,q-1}$", indicating the the projectile charge changes from q to q-1. To illustrate the composition of the q,q-1 cross section, we display it along with the single charge transfer and transfer ionization cross sections in Figure 19 to 21. The two components are roughly equal in magnitude, transfer ionization dominating at high energy and single charge transfer at low. Again for the Be^{2+} ion we have prevented capture to the closed n=1 level. Finally, state-selective cross sections are tabulated in Tables 16 to 30, and n resolved cross sections are displayed graphically in Figures 22 to 24.

5 Summary

Since beryllium is beginning to play and important role as a low-Z plasma facing material in present and planned fusion energy devices, an extensive database of inelastic cross sections over a range of energies pertaining to the edge and central plasmas must be assembled for modeling and diagnostic purposes. To this end, we have presented cross sections for ionization, excitation, and charge transfer processes in 1 to 1000 keV/u collisions of $Be^{2,3,4+}$ + H and H_2. Cross sections have been presented graphically for all these processes and compared with existing data to aid in the assessment of the limits of validity of the theoretical method used to provide this broad range of results. Furthermore, state-selective (n, ℓ resolved) cross sections have been tabulated for charge transfer owing to the need for these data in charge exchange recombination spectroscopy.

6 Acknowledgement

The authors gratefully acknowledge the support for this work from the US Department of Energy, Office of Fusion Energy, through contract number DE-AC05-84OR21400 with Oak Ridge National Laboratory, managed by Lockheed Martin Energy Systems, Inc.

References

[1] "Atomic and Molecular Processes in Fusion Edge Plasmas," R.K. Janev, editor (Plenum Press, New York, 1995).

[2] R.E. Olson and D.R. Schultz, Physica Scripta **T28**, 71 (1989).

[3] D.R. Schultz, L. Meng, C.O. Reinhold, and R.E. Olson, Physica Scripta **T37**, 89 (1991).

[4] R. Abrines and I.C. Percival, Proc. Phys. Soc. London **88**, 861 (1966).

[5] R.E. Olson and A. Salop, Phys. Rev. A **16**, 531 (1977).

[6] C.O. Reinhold, R.E. Olson, and W. Fritsch, Phys. Rev. A **41**, 4837 (1990).

[7] R.L. Becker and A.D. MacKellar, J. Phys. B **17**, 3923 (1984).

[8] L. Meng, C.O. Reinhold, and R.E. Olson, Phys. **40**, 3637 (1989); Phys. Rev. A **42**, 5286 (1990).

[9] G. Peach, S.L. Willis, and M.R.C. McDowell, J. Phys. B **18**, 3921 (1985); S.L. Willis, G. Peach, M.R.C. McDowell, and J. Banerji, J. Phys. B **18**, 3939 (1985).

[10] L.H. Toburen, R.D. DuBois, C.O. Reinhold, D.R. Schultz, and R.E. Olson, Phys. Rev. A **42**, 5338 (1990).

[11] P.S. Krstić, M. Radmilovic, and R.K. Janev, Atomic and Plasma-Material Interaction Data for Fusion (Supplement to the journal Nuclear Fusion) **3**, 113 (1992).

[12] W. Fritsch, in *Proceedings of the VIth International Conference on the Physics of Highly Charged Ions*, P. Richard *et al.*, editors (American Institute of Physics, New York, 1993), p. 24.

[13] W. Fritsch, in *Review of Fundamental Processes and Applications of Atoms and Ions*, C.D. Lin, editor (World Scientific, Singapore, 1993), p. 239.

[14] M.B. Shah and H.B. Gilbody, J. Phys. B **15**, 3441 (1982).

[15] M. Kimura as cited in [11] (1992).

[16] R.K. Janev, H.P Winter, and W. Fritsch, in *Atomic and Molecular Processes in Fusion Edge Plasmas*, R.K. Janev, Editor (Plenum, New York, 1995) p. 341.

[17] A.E. Wetmore, H.R. Cole, and R.E. Olson, J. Phys. B **19**, 1515 (1986).

[18] D.R. Bates and B.L. Moiseiwitsch, Proc. Phys. Soc. **67**, 805 (1954).

[19] N. Shimakura, J. Phys. B **21**, 2485 (1988).

[20] R. Olson, Phys. Rev. A bf 24, 1726 (1981).

[21] M. Kimura, quoted in Ref. [16] (1995).

7 Figure Captions

Figure 1. Comparison of the present CTMC result with that from Ref. [11] for the hidden crossing (HC) method regarding ionization of H by Be^{4+} impact.

Figure 2. CTMC results for ionization in Be^{q+} + H.

Figure 3. CTMC results for ionization in $Be^{4+} + H_2$. Denoted are the single, double, and transfer ionization components of the free electron production cross section.

Figure 4. Same as Figure 3 except for $Be^{3+} + H_2$.

Figure 5. Same as Figure 3 except for $Be^{2+} + H_2$.

Figure 6. Comparison of theories regarding excitation to H(n=2) and H(n=3) in collisions of Be^{4+} with atomic hydrogen. AO_1 labels the atomic orbital close coupling calculation of Fritsch as quoted in Ref. [11] and AO_2 labels those from Ref. [12]. The HC calculations are from Ref. [11].

Figure 7. CTMC results for excitation to various n, ℓ and n states of H in collisions of Be^{4+} with atomic hydrogen.

Figure 8. Same as Figure 7 except for Be^{3+} + H.

Figure 9. Same as Figure 7 except for Be^{2+} + H.

Figure 10. Dissociative capture, dissociation, and dissociative ionization in collisions of Be^{q+} with H_2 computed using the CTMC technique. The symbols in parentheses give the final products in each case for clarity.

Figure 11. Comparison of the existing theories for charge transfer in Be^{4+} + H. HC labels the hidden crossing result [11], AO_2 the AO calculation of Fritsch [12], MO the molecular orbital calculation of Kimura [15], "rec" is the recommended cross section given by Janev *et al.* [16], and CTMC is the present result.

Figure 12. Comparison of the existing theories for charge transfer in $Be^{3,2+}$ + H. PSS labels the perturbed stationary state calculations of Wetmore *et al.* [17], L-Z the Landau-Zener results of Bates and Moiseiwitsch [18], and MO the molecular orbital calculations of Shimakura [19].

Figure 13. The CTMC result for total charge transfer in collisions of Be^{q+} + H.

Figure 14. Comparison of the existing theories for n-level resolved charge transfer in Be^{4+} + H collisions. The solid curves are CTMC results, the dashed curve is the result of the HC model [11], and the chain dashed curve represent the AO calculations of Fritsch [12]. The numbers label the particular n-levels for each theory.

Figure 15. The CTMC results for charge transfer resolved by n-level in $Be^{4+} + H$ collisions.

Figure 16. The same as Figure 15 except for $Be^{3+} + H$.

Figure 17. The same as Figure 15 except for $Be^{2+} + H$.

Figure 18. Comparison of the atomic orbital – molecular orbital (AO-MO) calculations of Kimura [21] with the present CTMC results for single charge transfer in $Be^{4,3,2+} + H_2$.

Figure 19. The CTMC result for charge transfer for $Be^{4+} + H_2$: solid curve is for the so-called "q, q-1" cross section which is the sum of single charge transfer (dashed curve) and transfer ionization (dotted curve).

Figure 20. The same as Figure 19 except for $Be^{3+} + H_2$.

Figure 21. The same as Figure 19 except for $Be^{2+} + H_2$.

Figure 22. The CTMC result for the q, q-1 cross section (sum of single charge transfer and transfer ionization) for $Be^{4+} + H_2$ resolved by n-levels.

Figure 23. The same as Figure 22 except for $Be^{3+} + H_2$.

Figure 24. The same as Figure 22 except for $Be^{2+} + H_2$.

Figure 1:

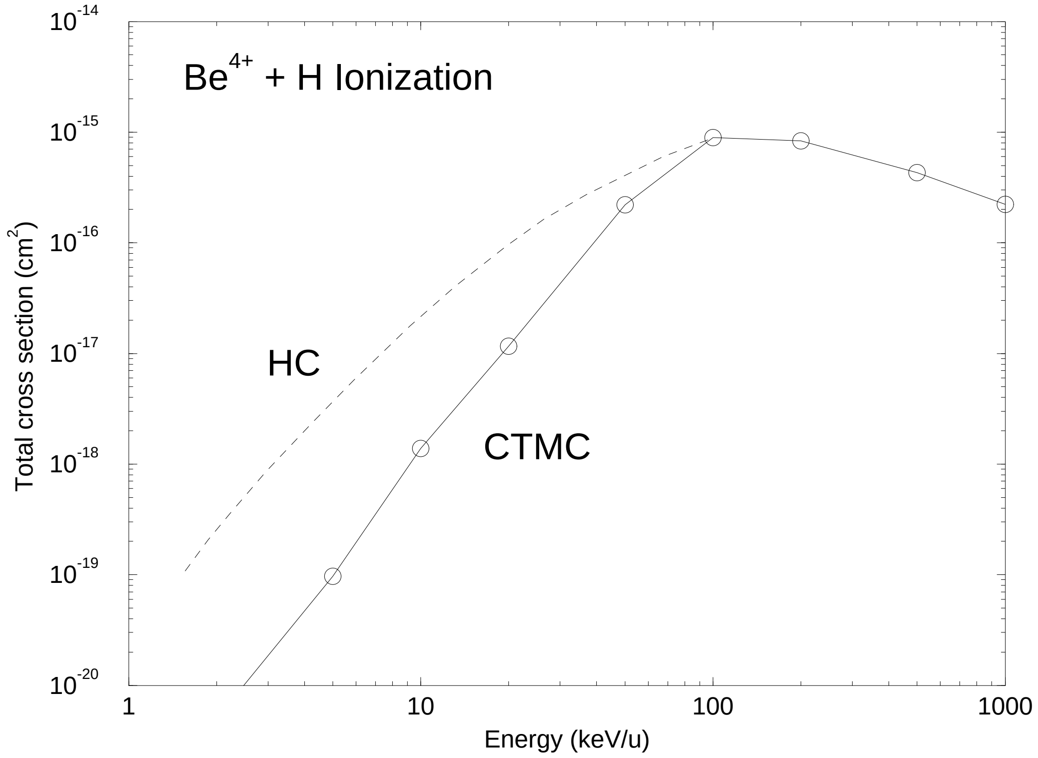

Be4+ + H Ionization
HC
CTMC
Total cross section (cm2)
Energy (keV/u)
10-14
10-15
10-16
10-17
10-18
10-19
10-20
1
10
100
1000

Figure 2:

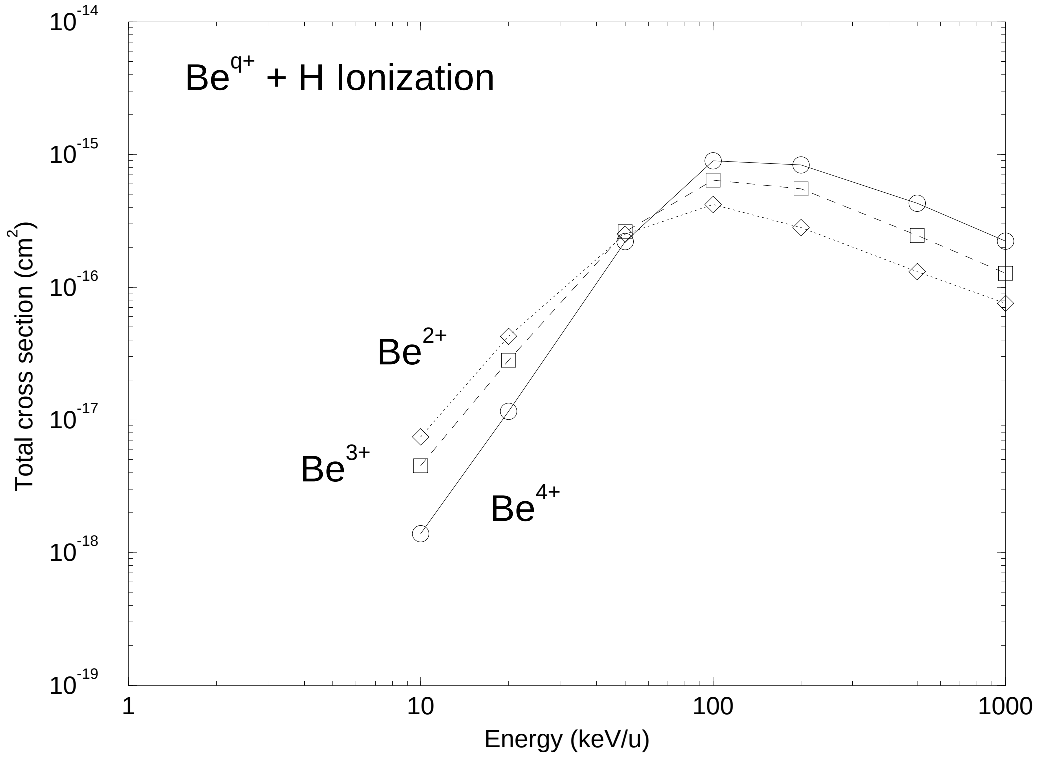

Be^{q+} + H Ionization
Be^{2+}
Be^{3+}
Be^{4+}
Total cross section (cm^2)
10^{-14}
10^{-15}
10^{-16}
10^{-17}
10^{-18}
10^{-19}
1
10
100
1000
Energy (keV/u)

Figure 3:

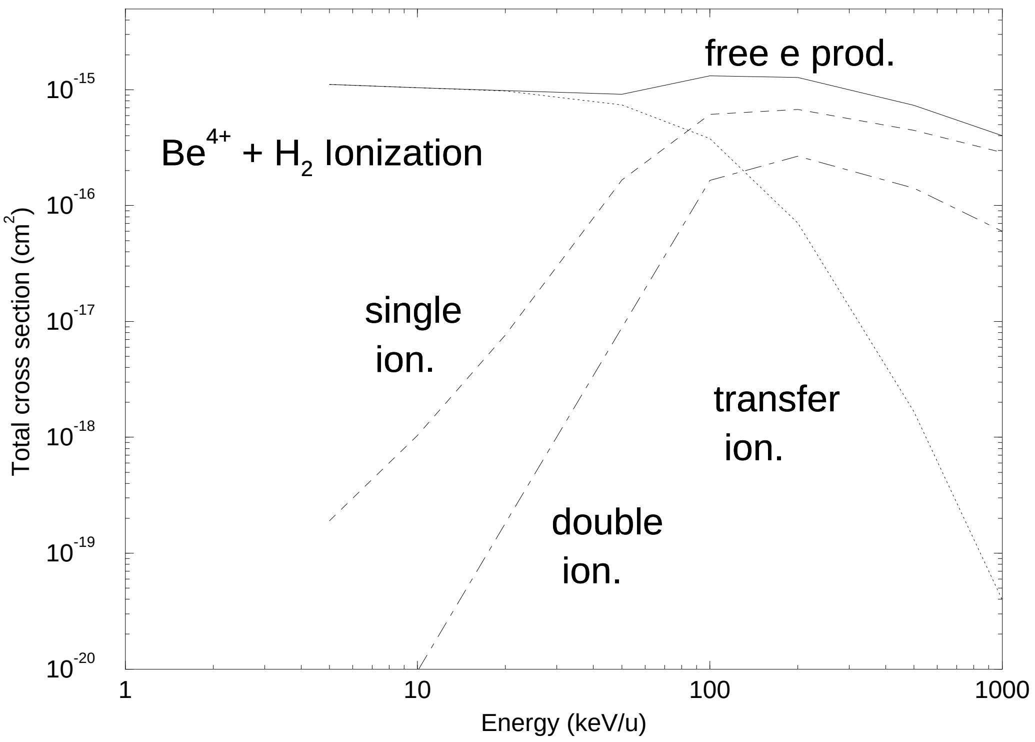

free e prod.
Be4+ + H2 Ionization
single
ion.
transfer
ion.
double
ion.
Total cross section (cm2)
Energy (keV/u)
10-15
10-16
10-17
10-18
10-19
10-20
1
10
100
1000

Figure 4:

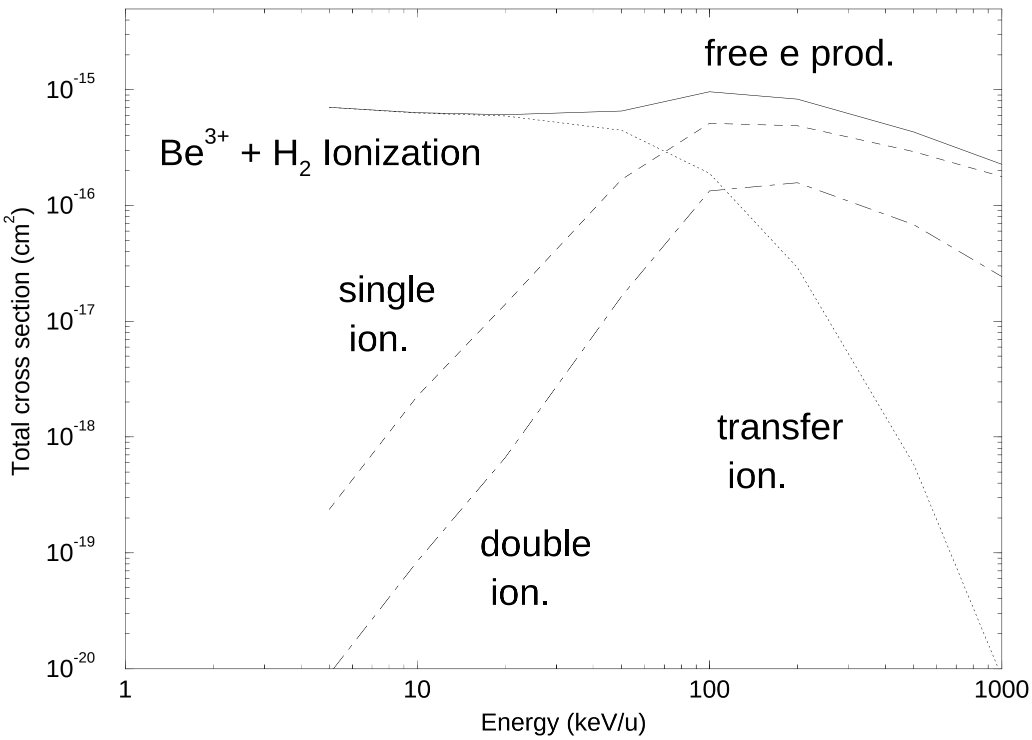

free e prod.
Be^{3+} + H$_2$ Ionization
single ion.
transfer ion.
double ion.
Total cross section (cm^2)
Energy (keV/u)
10^{-15}
10^{-16}
10^{-17}
10^{-18}
10^{-19}
10^{-20}
1
10
100
1000

Figure 5:

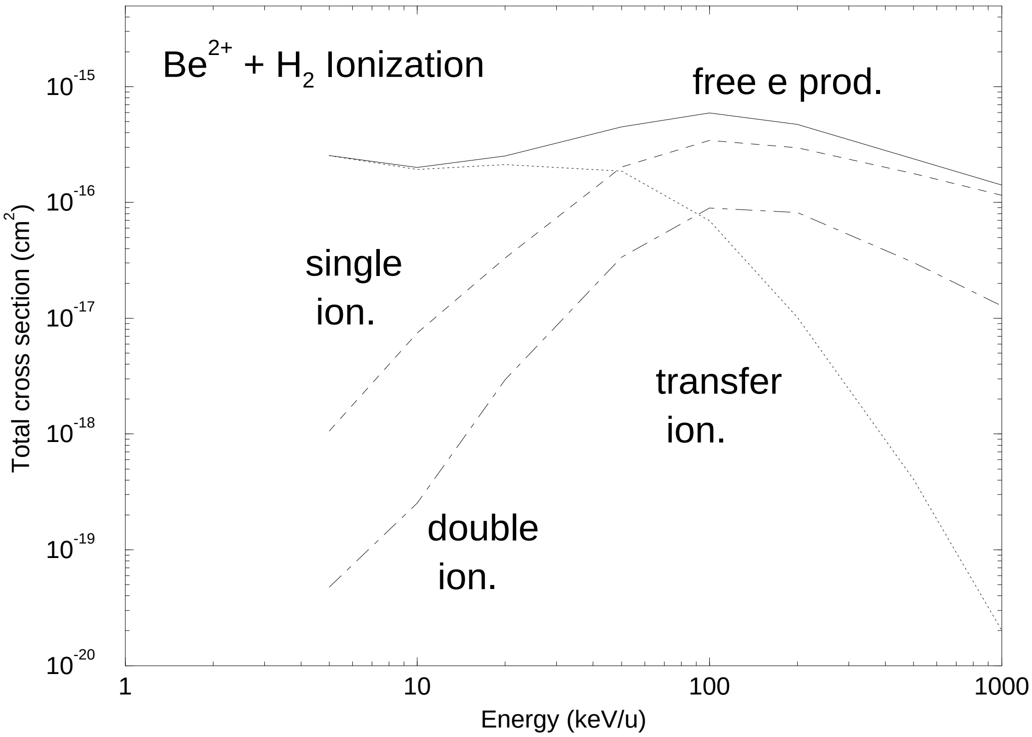

Be^{2+} + H$_2$ Ionization
free e prod.
single ion.
transfer ion.
double ion.
Total cross section (cm^2)
Energy (keV/u)
10^{-15}
10^{-16}
10^{-17}
10^{-18}
10^{-19}
10^{-20}
1
10
100
1000

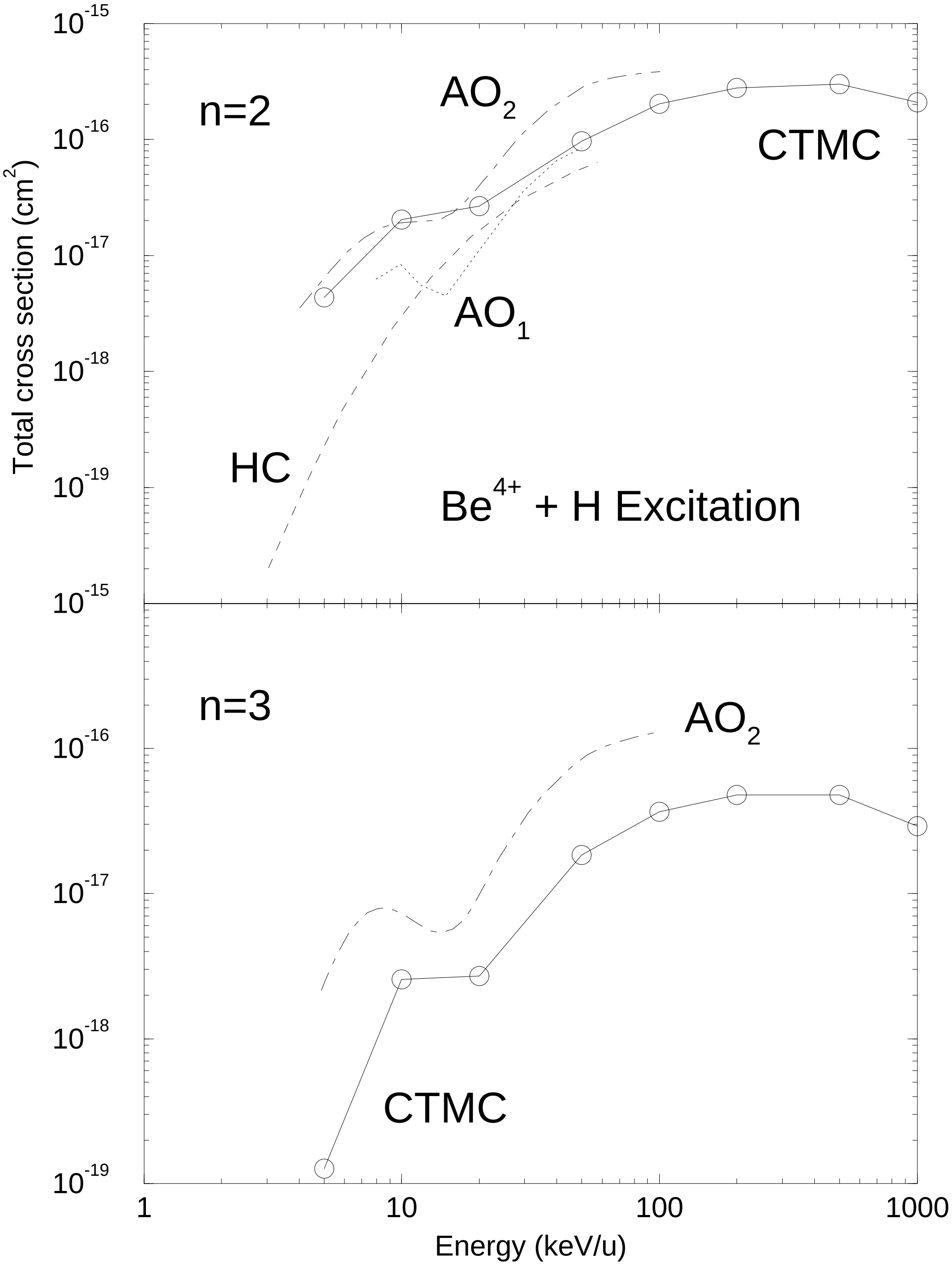

n=2
AO$_2$
CTMC
AO$_1$
HC
Be^{4+} + H Excitation
n=3
AO$_2$
CTMC
Total cross section (cm^2)
Energy (keV/u)
10^{-15}
10^{-16}
10^{-17}
10^{-18}
10^{-19}
1
10
100
1000

Figure 6:

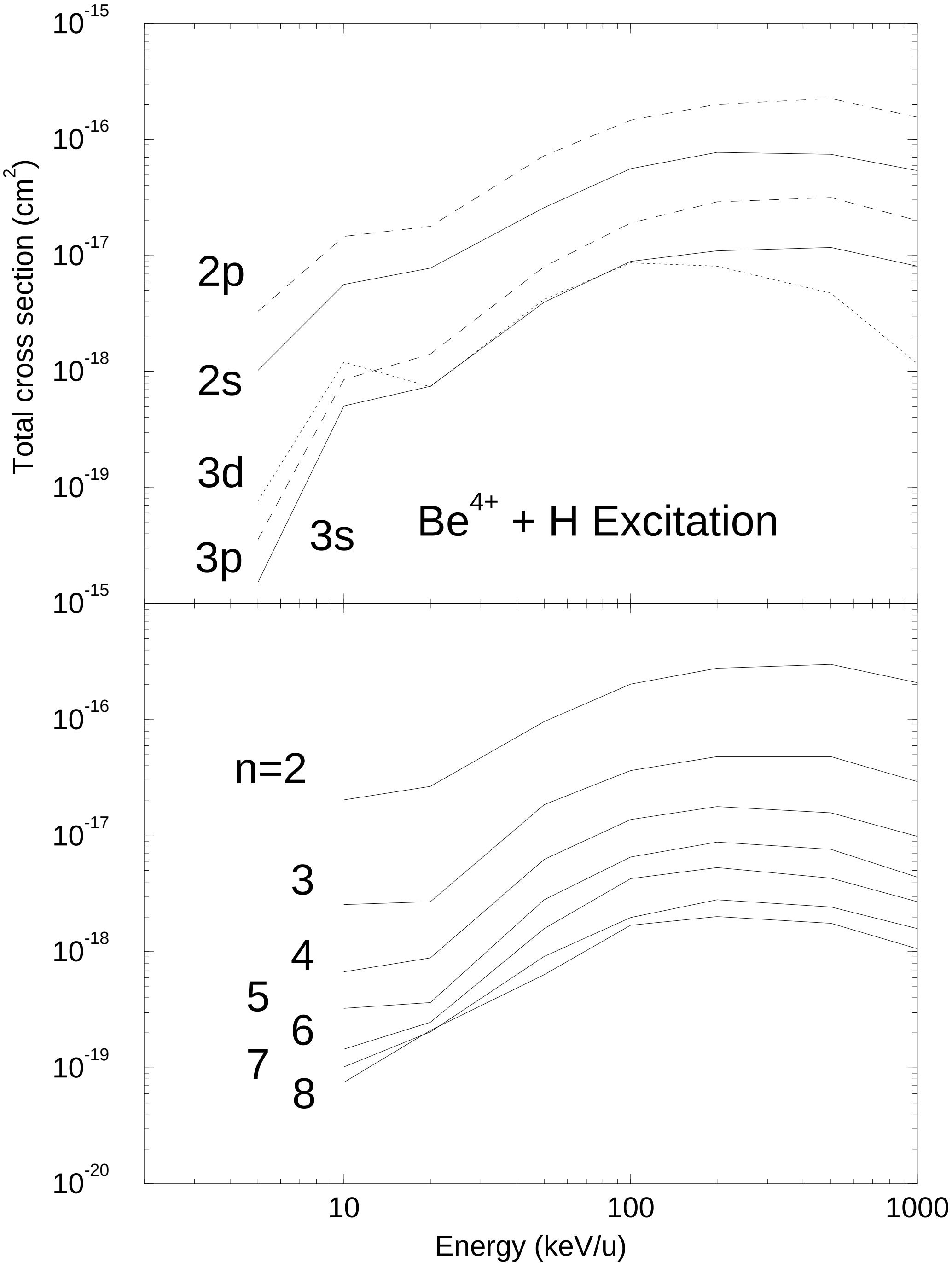

Be^{4+} + H Excitation
2p
2s
3d
3p
3s
n=2
3
4
5
6
7
8
Total cross section (cm^2)
Energy (keV/u)
10^{-15}
10^{-16}
10^{-17}
10^{-18}
10^{-19}
10^{-20}
10
100
1000

Figure 7:

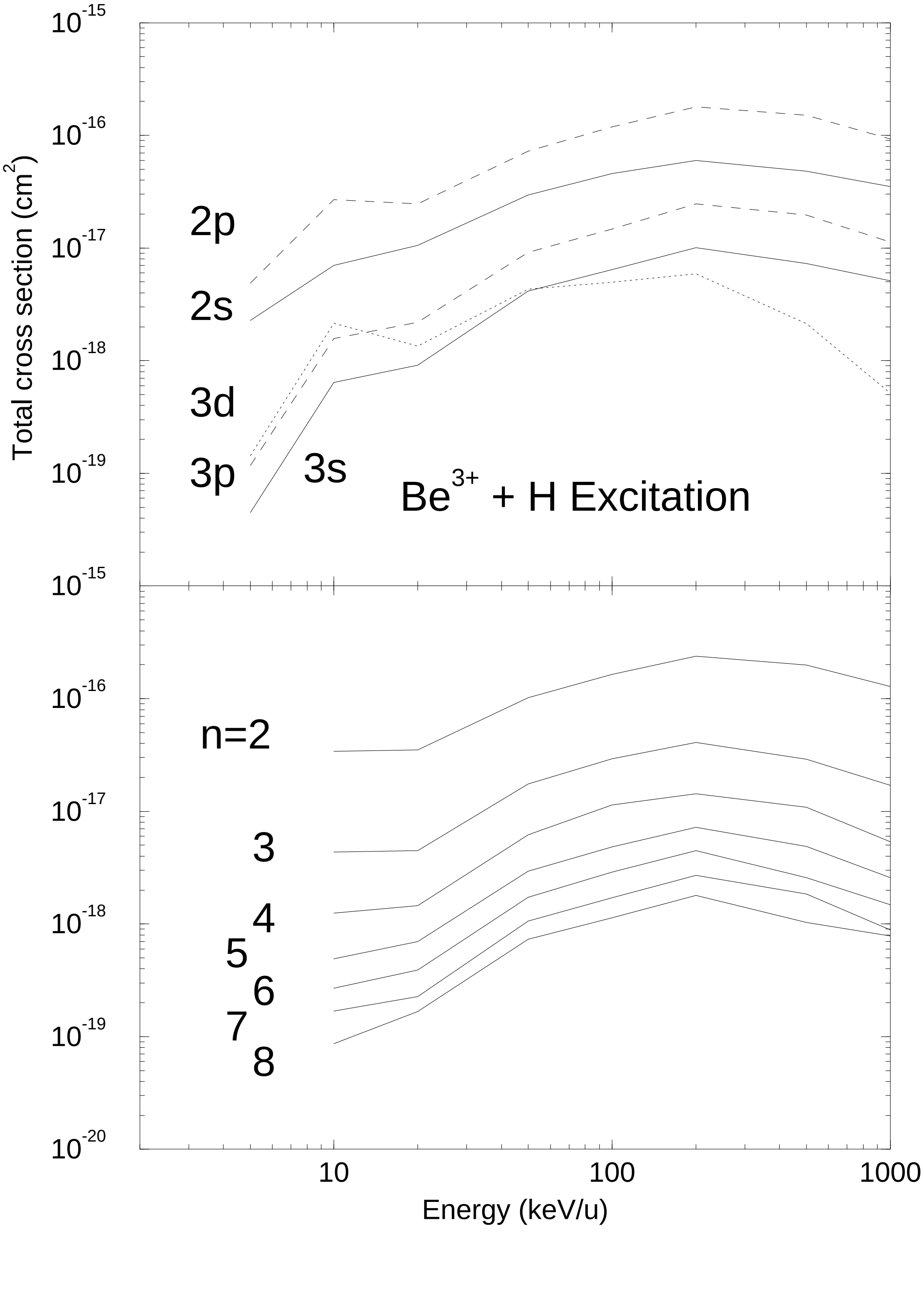
Be^{3+} + H Excitation
2p
2s
3d
3p
3s
n=2
3
4
5
6
7
8
Total cross section (cm^2)
Energy (keV/u)
10^{-15}
10^{-16}
10^{-17}
10^{-18}
10^{-19}
10^{-20}
10
100
1000

Figure 8:

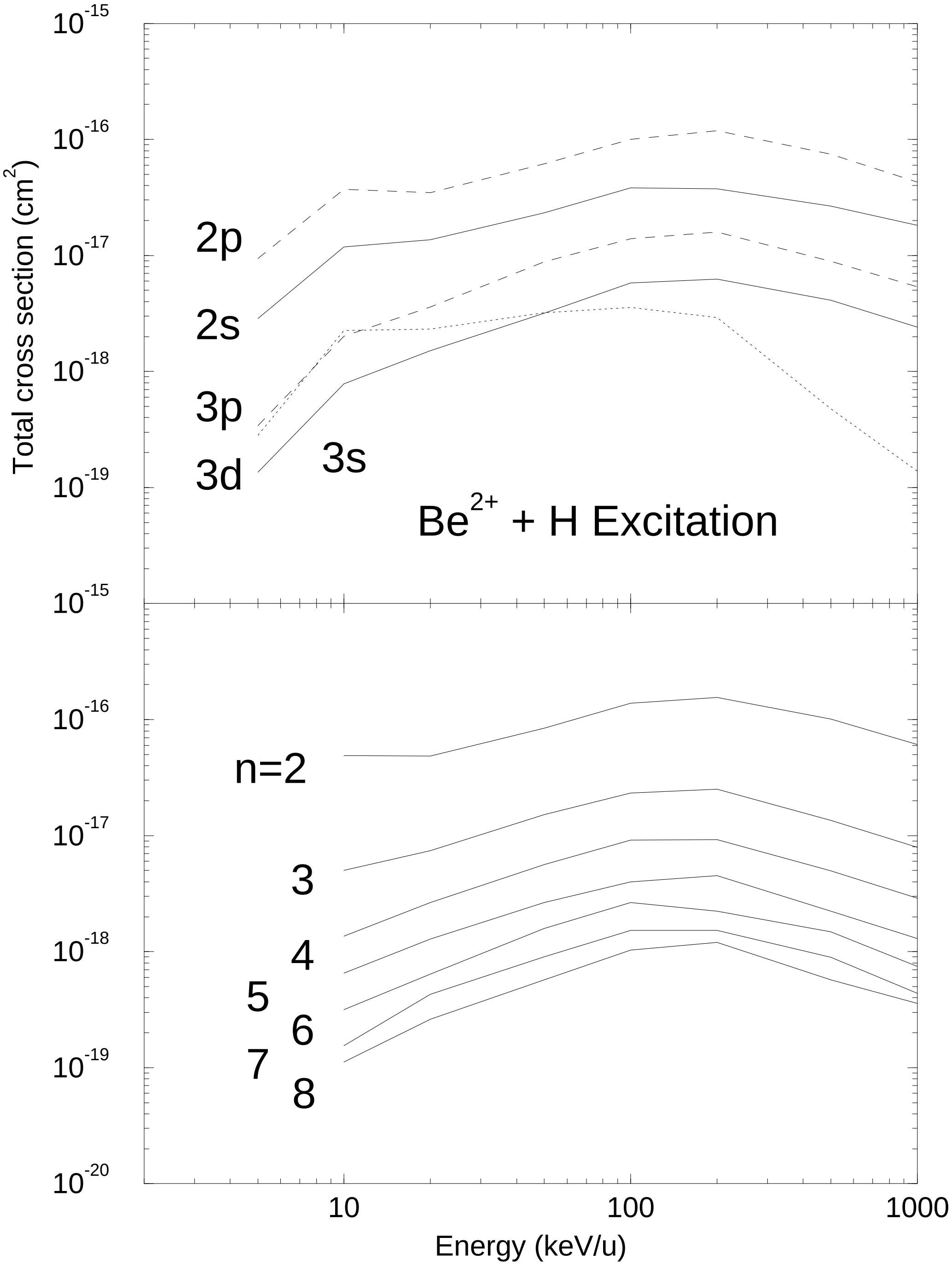

Be^{2+} + H Excitation
2p
2s
3p
3d
3s
n=2
3
4
5
6
7
8
Total cross section (cm^2)
Energy (keV/u)
10
100
1000
10^{-15}
10^{-16}
10^{-17}
10^{-18}
10^{-19}
10^{-20}

Figure 9:

Figure 10:

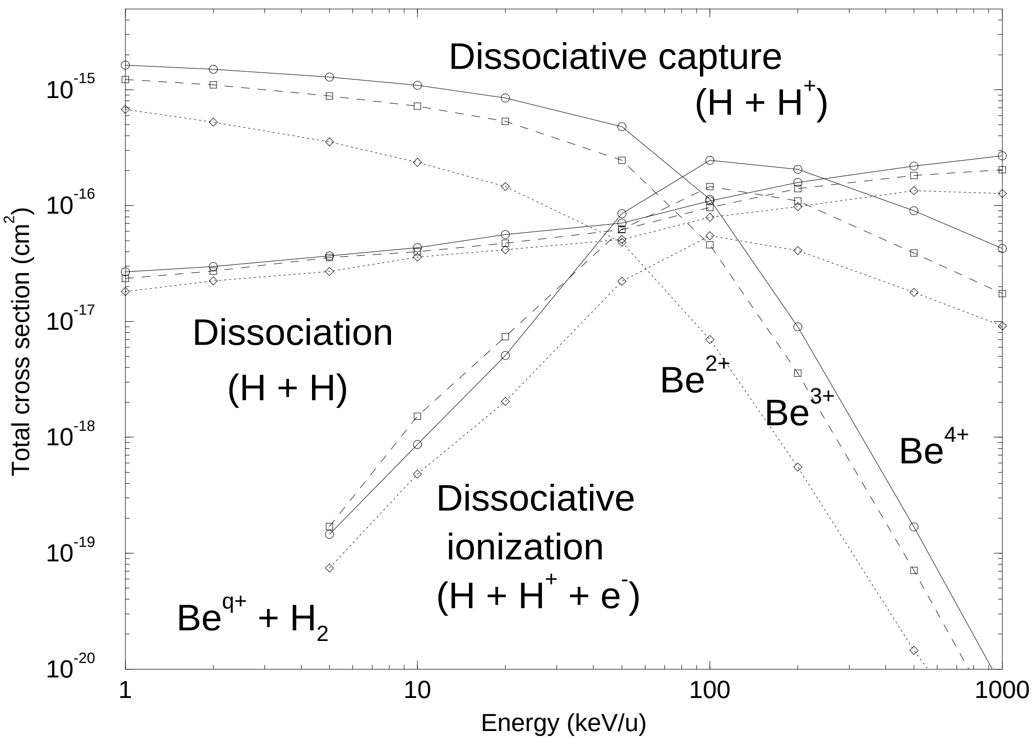

Dissociative capture
(H + H+)
Dissociation
(H + H)
Be2+
Be3+
Be4+
Dissociative
ionization
(H + H+ + e-)
Beq+ + H2
Total cross section (cm2)
Energy (keV/u)
10-15
10-16
10-17
10-18
10-19
10-20
1
10
100
1000

Figure 11:

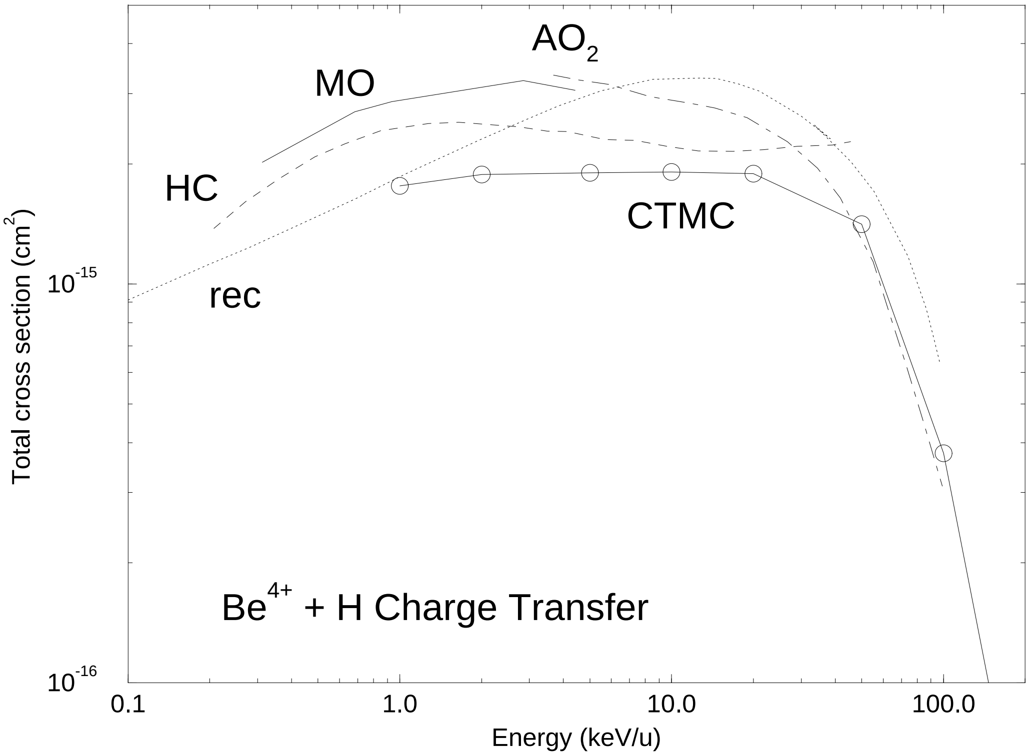

AO$_2$
MO
HC
CTMC
rec
Be^{4+} + H Charge Transfer
Total cross section (cm^2)
10^{-15}
10^{-16}
0.1
1.0
10.0
100.0
Energy (keV/u)

Figure 12:

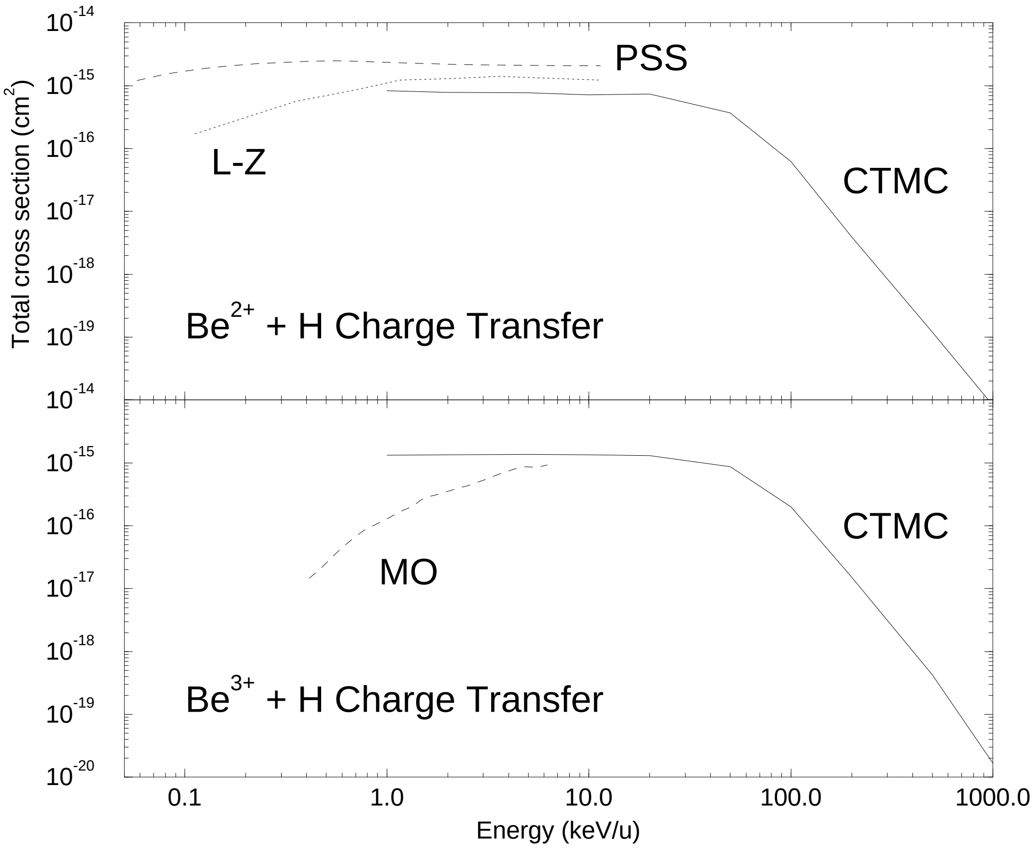
PSS
L-Z
CTMC
Be2+ + H Charge Transfer
MO
CTMC
Be3+ + H Charge Transfer
Total cross section (cm2)
Energy (keV/u)
0.1
1.0
10.0
100.0
1000.0

Figure 13:

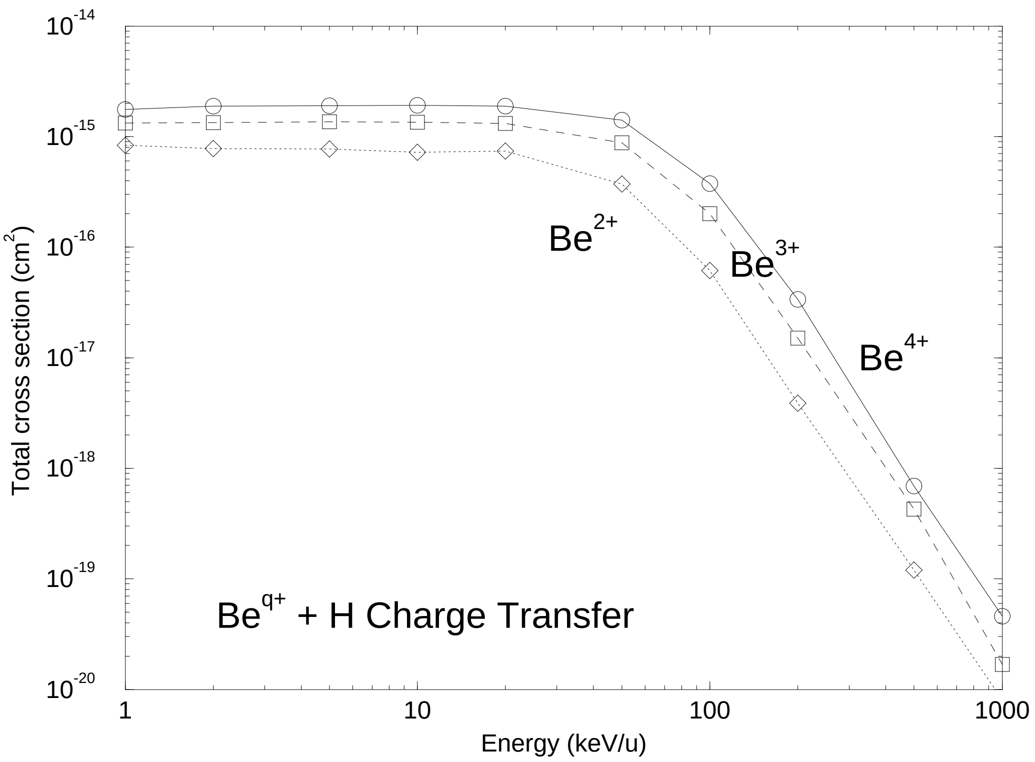

10-14
10-15
10-16
10-17
10-18
10-19
10-20
Total cross section (cm2)
1
10
100
1000
Energy (keV/u)
Be2+
Be3+
Be4+
Beq+ + H Charge Transfer

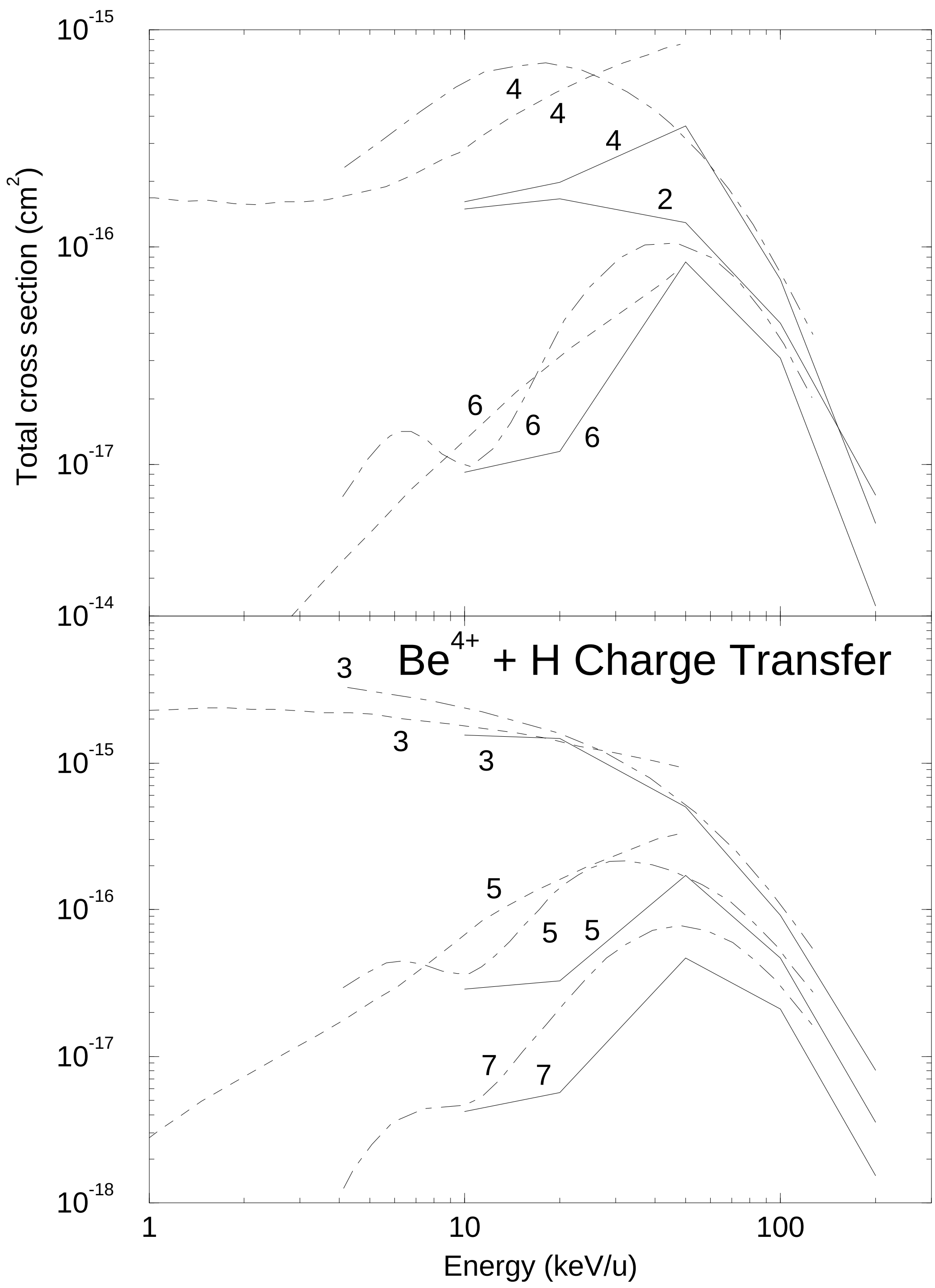

Be^{4+} + H Charge Transfer
Total cross section (cm^2)
Energy (keV/u)
10^{-15}
10^{-16}
10^{-17}
10^{-14}
10^{-18}
1
10
100
4
4
4
2
6
6
6
3
3
3
5
5
5
7
7

Figure 14:

Figure 15:

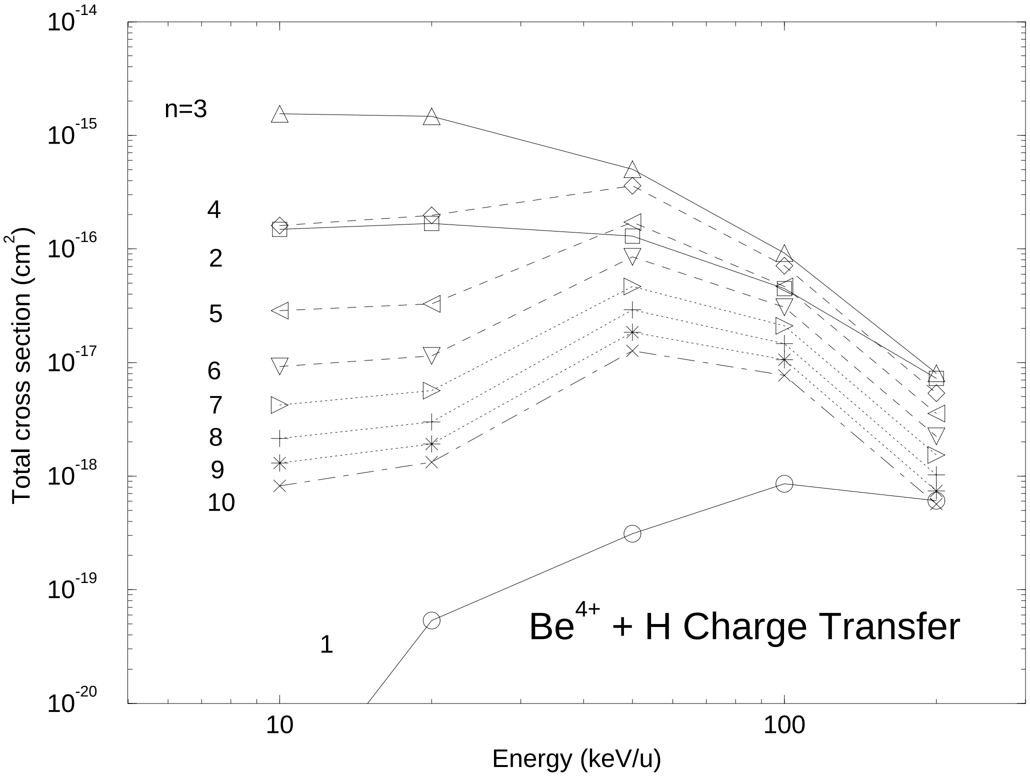

10^{-14}
10^{-15}
10^{-16}
10^{-17}
10^{-18}
10^{-19}
10^{-20}
Total cross section (cm^2)
n=3
4
2
5
6
7
8
9
10
1
Be^{4+} + H Charge Transfer
10
100
Energy (keV/u)

Figure 16:

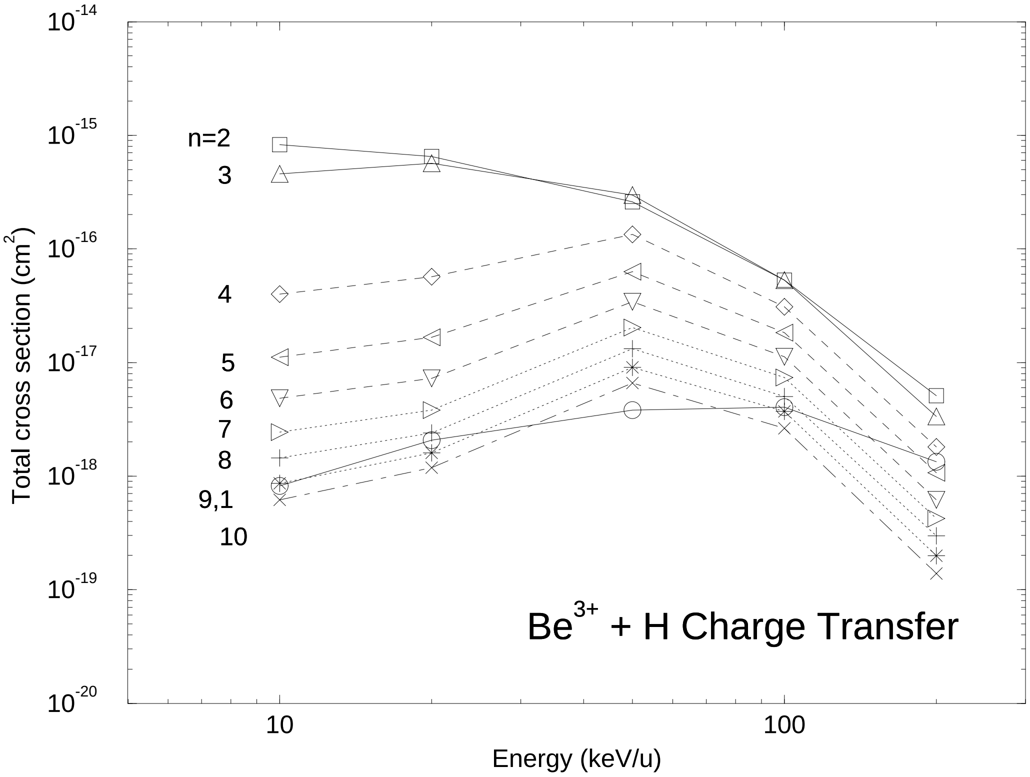

10^-14
10^-15
10^-16
10^-17
10^-18
10^-19
10^-20
Total cross section (cm^2)
n=2
3
4
5
6
7
8
9,1
10
Be^3+ + H Charge Transfer
10
100
Energy (keV/u)

Figure 17:

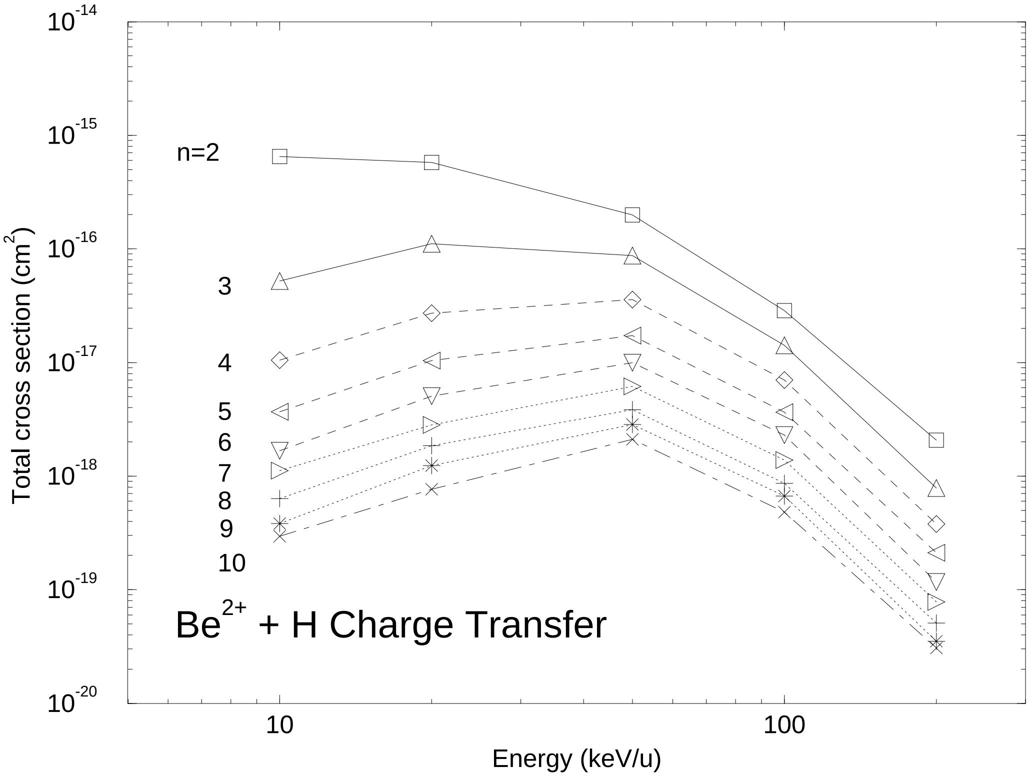

Be2+ + H Charge Transfer
n=2
3
4
5
6
7
8
9
10
Total cross section (cm2)
Energy (keV/u)
10-14
10-15
10-16
10-17
10-18
10-19
10-20
10
100

Figure 18:

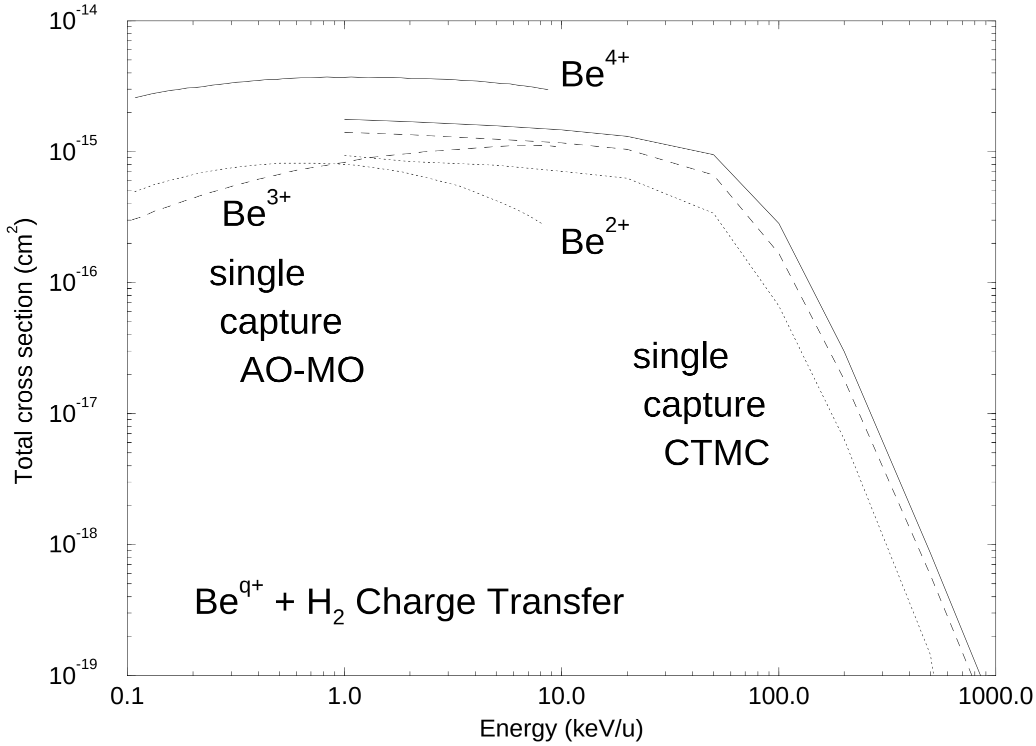
10^{-14}
10^{-15}
10^{-16}
10^{-17}
10^{-18}
10^{-19}
Total cross section (cm^2)
Be^{4+}
Be^{3+}
Be^{2+}
single
capture
AO-MO
single
capture
CTMC
$Be^{q+} + H_2$ Charge Transfer
0.1
1.0
10.0
100.0
1000.0
Energy (keV/u)

Figure 19:

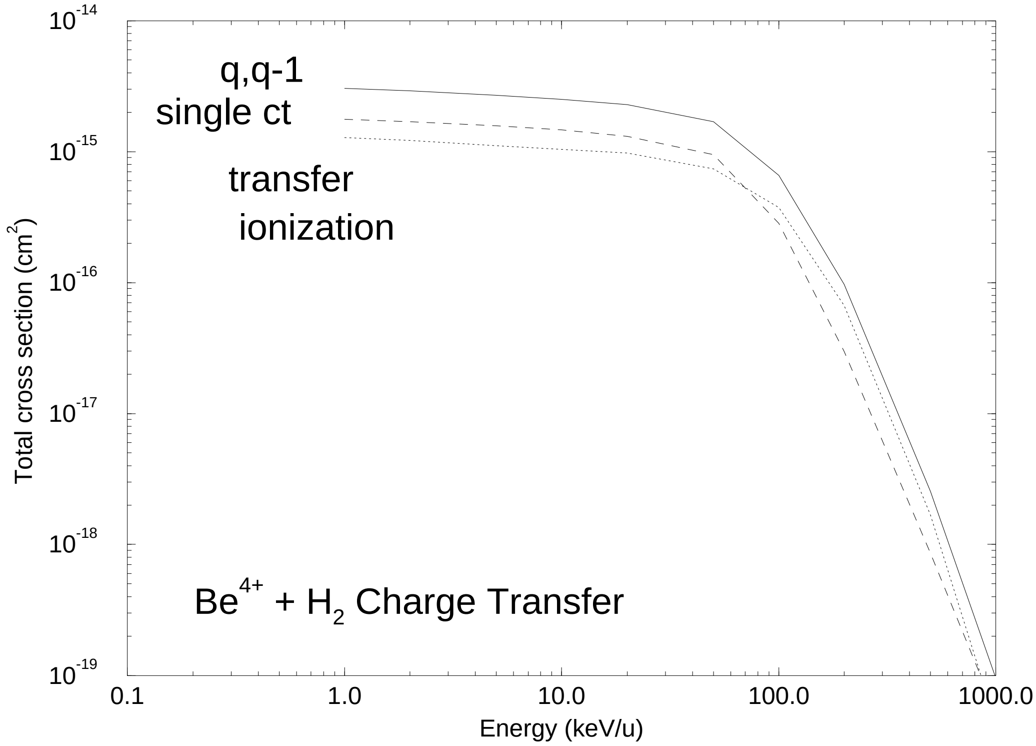

q,q-1
single ct
transfer
ionization
Be^{4+} + H$_2$ Charge Transfer
Total cross section (cm^2)
Energy (keV/u)
10^{-14}
10^{-15}
10^{-16}
10^{-17}
10^{-18}
10^{-19}
0.1
1.0
10.0
100.0
1000.0

Figure 20:

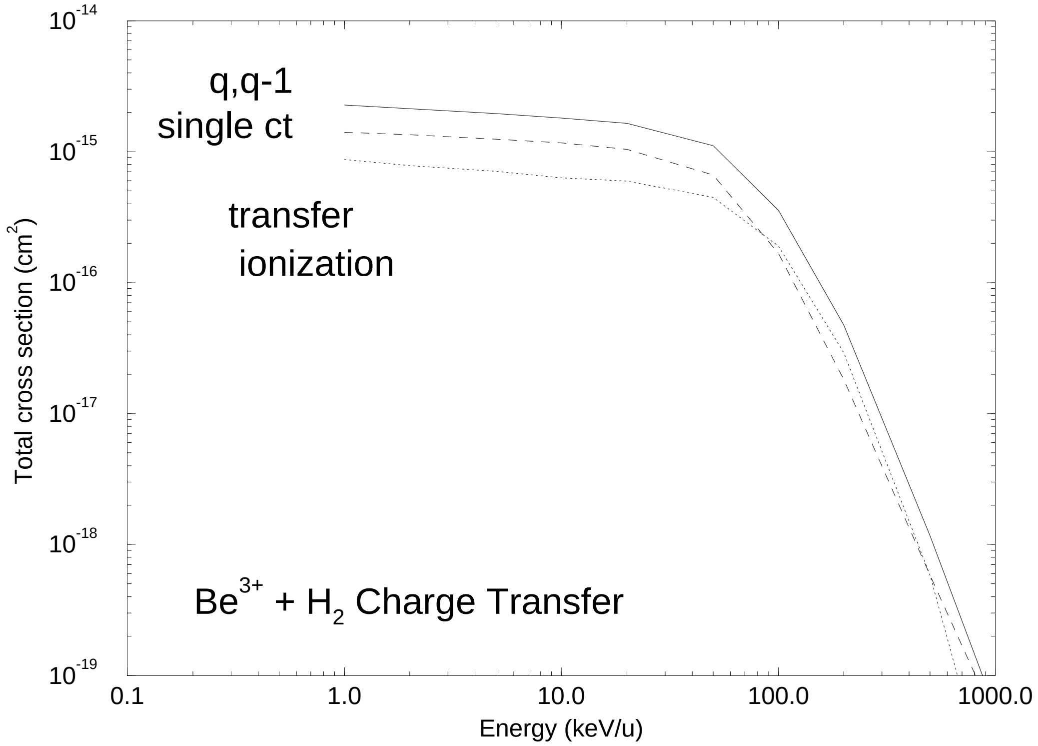

q,q-1
single ct
transfer
ionization
Be3+ + H2 Charge Transfer
Total cross section (cm2)
Energy (keV/u)
10-14
10-15
10-16
10-17
10-18
10-19
0.1
1.0
10.0
100.0
1000.0

Figure 21:

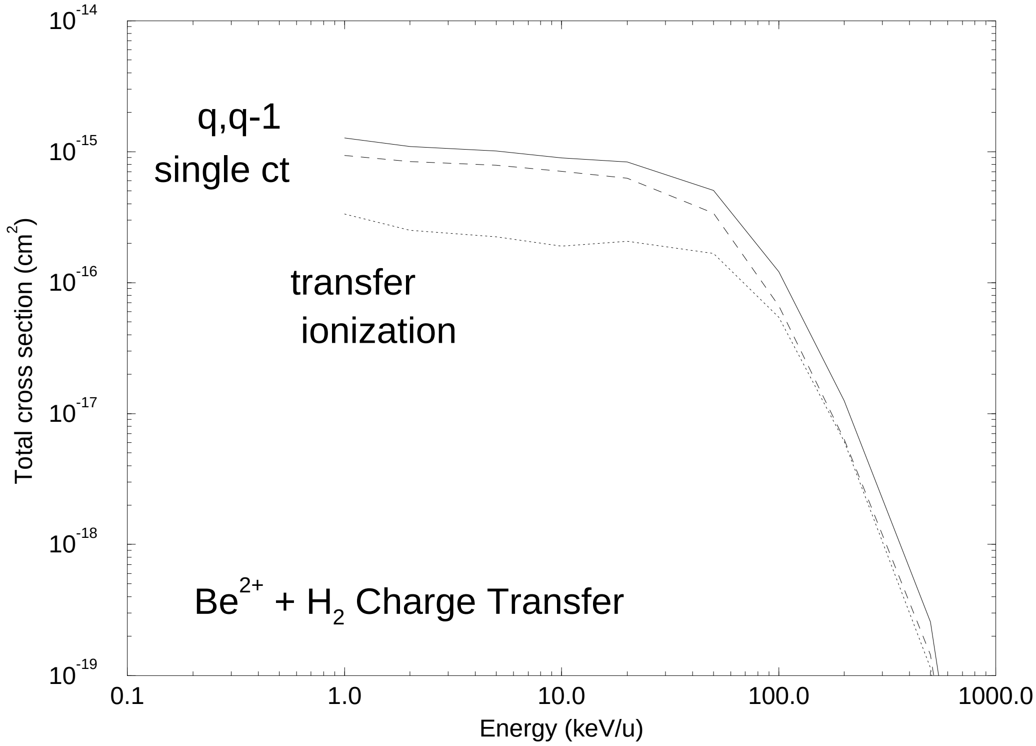

10^{-14}
10^{-15}
10^{-16}
10^{-17}
10^{-18}
10^{-19}
Total cross section (cm^2)
q,q-1
single ct
transfer
ionization
$Be^{2+} + H_2$ Charge Transfer
0.1
1.0
10.0
100.0
1000.0
Energy (keV/u)

Figure 22:

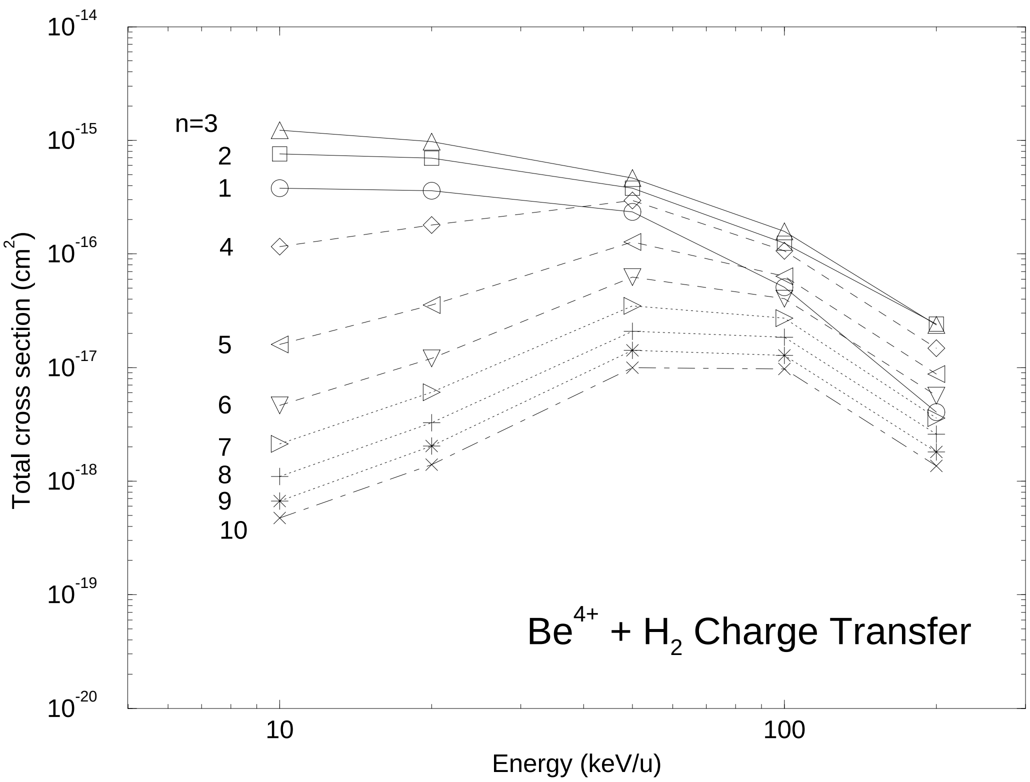

10^{-14}
10^{-15}
10^{-16}
10^{-17}
10^{-18}
10^{-19}
10^{-20}
Total cross section (cm^2)
n=3
2
1
4
5
6
7
8
9
10
$Be^{4+} + H_2$ Charge Transfer
10
100
Energy (keV/u)

Figure 23:

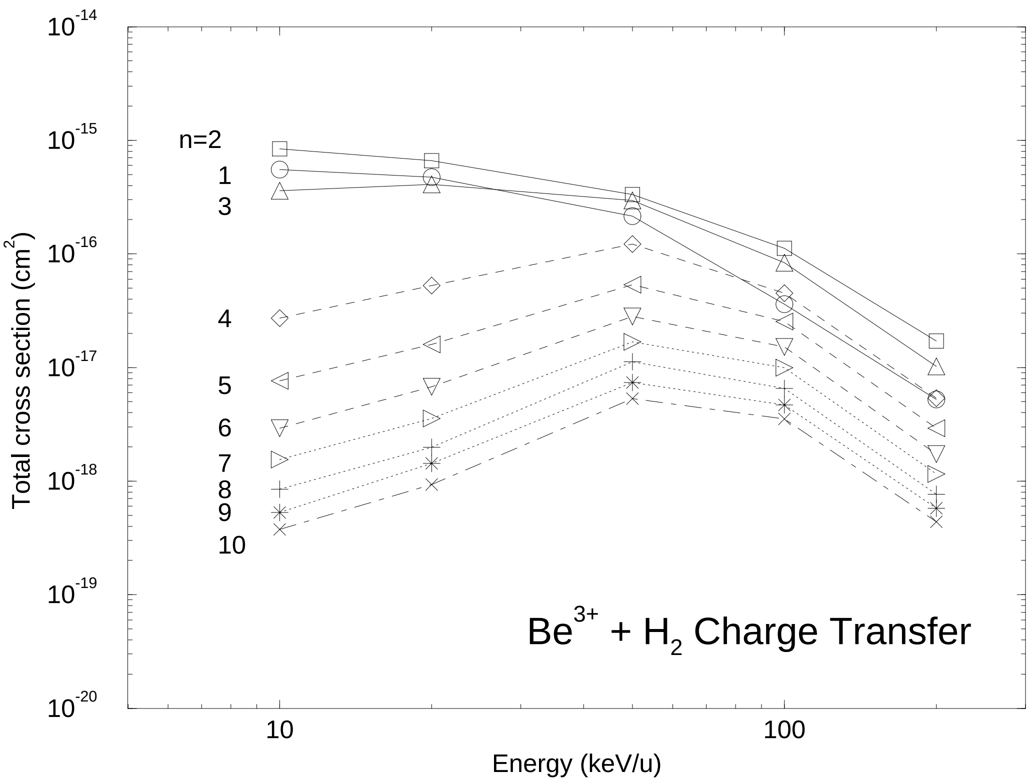

10^{-14}
10^{-15}
10^{-16}
10^{-17}
10^{-18}
10^{-19}
10^{-20}
Total cross section (cm^2)
n=2
1
3
4
5
6
7
8
9
10
$Be^{3+} + H_2$ Charge Transfer
10
100
Energy (keV/u)

Figure 24:

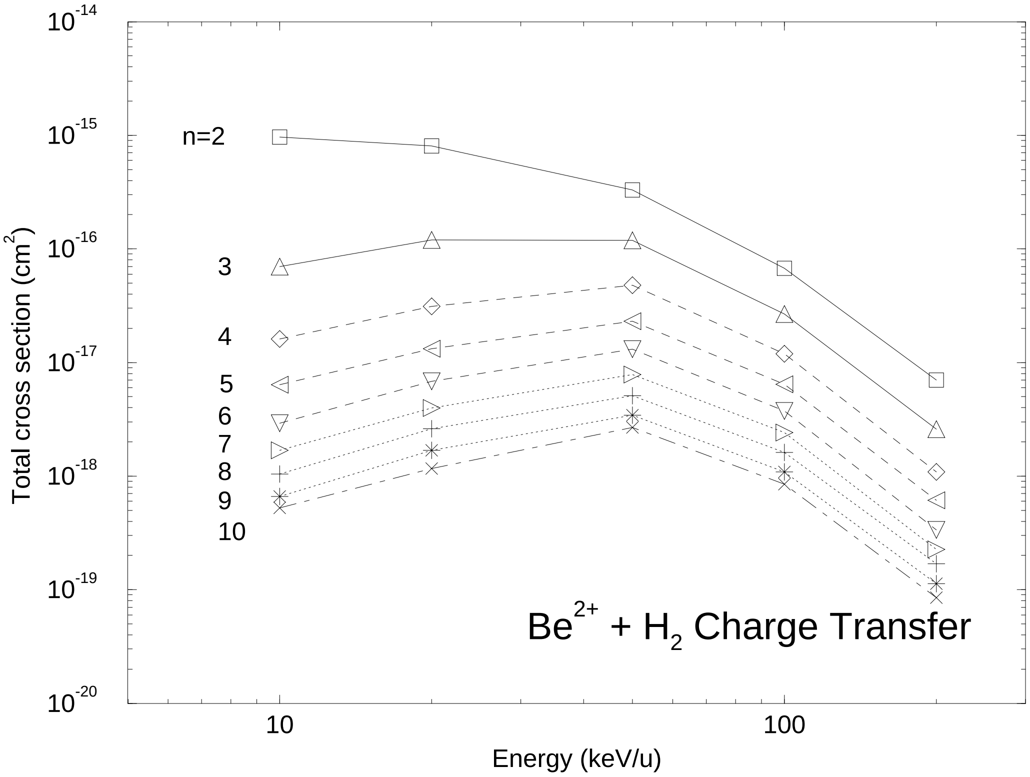

Be^{2+} + H$_2$ Charge Transfer
n=2
3
4
5
6
7
8
9
10
Total cross section (cm^2)
Energy (keV/u)
10^{-14}
10^{-15}
10^{-16}
10^{-17}
10^{-18}
10^{-19}
10^{-20}
10
100

n	ℓ	σ_{nl}	σ_n	σ
1	0			
2	0	4.23e-17	1.49e-16	
2	1	1.07e-16		
3	0	6.67e-17	1.55e-15	
3	1	3.30e-16		
3	2	1.15e-15		
4	0	1.67e-17	1.61e-16	
4	1	4.14e-17		
4	2	5.70e-17		
4	3	4.61e-17		
5	0	4.32e-18	2.87e-17	
5	1	8.06e-18		
5	2	8.25e-18		
5	3	5.87e-18		
5	4	2.21e-18		
6	Σ		9.20e-18	
7	Σ		4.21e-18	
8	Σ		2.14e-18	
9	Σ		1.31e-18	
10	Σ		8.19e-19	
Σ	Σ			1.91e-15

Table 1: CTMC cross sections for charge transfer in 10 keV Be^{4+} + H. The table includes the n, ℓ-distribution for $n \leq 5$, the n-distribution for $n \leq 10$, and the total charge transfer cross section for capture to all states. Cross sections are given in cm^2.

n	ℓ	σ_{nl}	σ_n	σ
1	0	5.35e-20	5.35e-20	
2	0	3.95e-17	1.67e-16	
2	1	1.27e-16		
3	0	3.20e-17	1.47e-15	
3	1	2.95e-16		
3	2	1.14e-15		
4	0	8.69e-18	1.98e-16	
4	1	3.34e-17		
4	2	7.42e-17		
4	3	8.15e-17		
5	0	3.70e-18	3.29e-17	
5	1	9.54e-18		
5	2	9.87e-18		
5	3	5.53e-18		
5	4	4.21e-18		
6	Σ		1.146e-17	
7	Σ		5.668e-18	
8	Σ		2.992e-18	
9	Σ		1.911e-18	
10	Σ		1.322e-18	
Σ	Σ			1.90e-15

Table 2: CTMC cross sections for charge transfer in 20 keV Be^{4+} + H. The table includes the n, ℓ-distribution for $n \leq 5$, the n-distribution for $n \leq 10$, and the total charge transfer cross section for capture to all states. Cross sections are given in cm^2.

n	ℓ	σ_{nl}	σ_n	σ
1	0	3.12e-19	3.12e-19	
2	0	1.92e-17	1.29e-16	
2	1	1.10e-16		
3	0	1.37e-17	5.03e-16	
3	1	1.07e-16		
3	2	3.82e-16		
4	0	8.26e-18	3.60e-16	
4	1	6.16e-17		
4	2	1.40e-16		
4	3	1.50e-16		
5	0	5.41e-18	1.72e-16	
5	1	3.55e-17		
5	2	6.68e-17		
5	3	6.02e-17		
5	4	3.76e-18		
6	Σ		8.53e-17	
7	Σ		4.67e-17	
8	Σ		2.90e-17	
9	Σ		1.84e-17	
10	Σ		1.27e-17	
Σ	Σ			1.41e-15

Table 3: CTMC cross sections for charge transfer in 50 keV Be^{4+} + H. The table includes the n, ℓ-distribution for $n \leq 5$, the n-distribution for $n \leq 10$, and the total charge transfer cross section for capture to all states. Cross sections are given in cm^2.

n	ℓ	σ_{nl}	σ_n	σ
1	0	8.52e-19	8.52e-19	
2	0	5.44e-18	4.47e-17	
2	1	3.92e-17		
3	0	3.89e-18	9.17e-17	
3	1	2.43e-17		
3	2	6.36e-17		
4	0	2.68e-18	7.10e-17	
4	1	1.47e-17		
4	2	3.05e-17		
4	3	2.31e-17		
5	0	1.76e-18	4.68e-17	
5	1	9.34e-18		
5	2	1.83e-17		
5	3	1.67e-17		
5	4	7.31e-19		
6	Σ		3.08e-17	
7	Σ		2.10e-17	
8	Σ		1.46e-17	
9	Σ		1.06e-17	
10	Σ		7.71e-18	
Σ	Σ			3.76e-16

Table 4: CTMC cross sections for charge transfer in 100 keV Be^{4+} + H. The table includes the n, ℓ-distribution for $n \leq 5$, the n-distribution for $n \leq 10$, and the total charge transfer cross section for capture to all states. Cross sections are given in cm^2.

n	ℓ	σ_{nl}	σ_n	σ
1	0	6.08e-19	6.08e-19	
2	0	1.16e-18	7.24e-18	
2	1	6.08e-18		
3	0	7.88e-19	8.05e-18	
3	1	3.23e-18		
3	2	4.03e-18		
4	0	4.93e-19	5.37e-18	
4	1	1.84e-18		
4	2	2.50e-18		
4	3	5.41e-19		
5	0	3.14e-19	3.57e-18	
5	1	1.23e-18		
5	2	1.53e-18		
5	3	4.85e-19		
5	4			
6	Σ		2.24e-18	
7	Σ		1.54e-18	
8	Σ		1.02e-18	
9	Σ		7.38e-19	
10	Σ		5.67e-19	
Σ	Σ			3.37e-17

Table 5: CTMC cross sections for charge transfer in 200 keV Be^{4+} + H. The table includes the n, ℓ-distribution for $n \leq 5$, the n-distribution for $n \leq 10$, and the total charge transfer cross section for capture to all states. Cross sections are given in cm^2.

n	ℓ	σ_{nl}	σ_n	σ
1	0	8.21e-19	8.21e-19	
2	0	2.01e-16	8.24e-16	
2	1	6.23e-16		
3	0	4.57e-17	4.58e-16	
3	1	1.29e-16		
3	2	2.83e-16		
4	0	6.36e-18	4.01e-17	
4	1	1.49e-17		
4	2	1.43e-17		
4	3	4.49e-18		
5	0	1.69e-18	1.11e-17	
5	1	3.99e-18		
5	2	3.08e-18		
5	3	2.02e-18		
5	4	3.33e-19		
6	Σ		4.83e-18	
7	Σ		2.43e-18	
8	Σ		1.45e-18	
9	Σ		8.62e-19	
10	Σ		6.20e-19	
Σ	Σ			1.35e-15

Table 6: CTMC cross sections for charge transfer in 10 keV Be^{3+} + H. The table includes the n, ℓ-distribution for $n \leq 5$, the n-distribution for $n \leq 10$, and the total charge transfer cross section for capture to all states. Cross sections are given in cm^2.

n	ℓ	σ_{nl}	σ_n	σ
1	0	2.07e-18	2.07e-18	
2	0	9.64e-17	6.50e-16	
2	1	5.54e-16		
3	0	2.62e-17	5.65e-16	
3	1	1.34e-16		
3	2	4.05e-16		
4	0	9.04e-18	5.71e-17	
4	1	1.80e-17		
4	2	1.38e-17		
4	3	1.63e-17		
5	0	3.02e-18	1.66e-17	
5	1	4.78e-18		
5	2	3.45e-18		
5	3	2.10e-18		
5	4	3.28e-18		
6	Σ		7.25e-18	
7	Σ		3.80e-18	
8	Σ		2.39e-18	
9	Σ		1.60e-18	
10	Σ		1.19e-18	
Σ	Σ			1.31e-15

Table 7: CTMC cross sections for charge transfer in 20 keV Be^{3+} + H. The table includes the n, ℓ-distribution for $n \leq 5$, the n-distribution for $n \leq 10$, and the total charge transfer cross section for capture to all states. Cross sections are given in cm^2.

n	ℓ	σ_{nl}	σ_n	σ
1	0	3.80e-18	3.80e-18	
2	0	2.87e-17	2.59e-16	
2	1	2.30e-16		
3	0	1.25e-17	2.98e-16	
3	1	1.02e-16		
3	2	1.83e-16		
4	0	7.70e-18	1.35e-16	
4	1	5.33e-17		
4	2	6.47e-17		
4	3	8.90e-18		
5	0	4.90e-18	6.28e-17	
5	1	2.87e-17		
5	2	2.61e-17		
5	3	3.09e-18		
5	4	3.72e-21		
6	Σ		3.43e-17	
7	Σ		2.03e-17	
8	Σ		1.33e-17	
9	Σ		9.09e-18	
10	Σ		6.60e-18	
Σ	Σ			8.70e-16

Table 8: CTMC cross sections for charge transfer in 50 keV Be^{3+} + H. The table includes the n, ℓ-distribution for $n \leq 5$, the n-distribution for $n \leq 10$, and the total charge transfer cross section for capture to all states. Cross sections are given in cm^2.

n	ℓ	σ_{nl}	σ_n	σ
1	0	4.06e-18	4.06e-18	
2	0	7.20e-18	5.31e-17	
2	1	4.59e-17		
3	0	4.36e-18	5.29e-17	
3	1	2.34e-17		
3	2	2.51e-17		
4	0	2.64e-18	3.10e-17	
4	1	1.33e-17		
4	2	1.41e-17		
4	3	9.36e-19		
5	0	1.60e-18	1.83e-17	
5	1	8.00e-18		
5	2	7.98e-18		
5	3	7.46e-19		
5	4			
6	Σ		1.12e-17	
7	Σ		7.40e-18	
8	Σ		5.02e-18	
9	Σ		3.71e-18	
10	Σ		2.64e-18	
Σ	Σ			2.01e-16

Table 9: CTMC cross sections for charge transfer in 100 keV Be^{3+} + H. The table includes the n, ℓ-distribution for $n \leq 5$, the n-distribution for $n \leq 10$, and the total charge transfer cross section for capture to all states. Cross sections are given in cm^2.

n	ℓ	σ_{nl}	σ_n	σ
1	0	1.34e-18	1.34e-18	
2	0	9.03e-19	5.10e-18	
2	1	4.20e-18		
3	0	4.81e-19	3.35e-18	
3	1	1.91e-18		
3	2	9.59e-19		
4	0	2.46e-19	1.81e-18	
4	1	1.03e-18		
4	2	5.34e-19		
4	3	1.80e-21		
5	0	1.51e-19	1.07e-18	
5	1	5.90e-19		
5	2	3.24e-19		
5	3			
5	4			
6	Σ		6.18e-19	
7	Σ		4.23e-19	
8	Σ		2.97e-19	
9	Σ		1.99e-19	
10	Σ		1.39e-19	
Σ	Σ			1.50e-17

Table 10: CTMC cross sections for charge transfer in 200 keV Be^{3+} + H. The table includes the n, ℓ-distribution for $n \leq 5$, the n-distribution for $n \leq 10$, and the total charge transfer cross section for capture to all states. Cross sections are given in cm^2.

n	ℓ	σ_{nl}	σ_n	σ
1	0			
2	0	1.82e-16	6.49e-16	
2	1	4.67e-16		
3	0	1.01e-17	5.23e-17	
3	1	2.45e-17		
3	2	1.77e-17		
4	0	1.76e-18	1.05e-17	
4	1	4.29e-18		
4	2	3.43e-18		
4	3	9.81e-19		
5	0	5.58e-19	3.69e-18	
5	1	1.14e-18		
5	2	1.16e-18		
5	3	7.47e-19		
5	4	8.45e-20		
6	Σ		1.68e-18	
7	Σ		1.12e-18	
8	Σ		6.32e-19	
9	Σ		3.82e-19	
10	Σ		2.94e-19	
Σ	Σ			7.21e-16

Table 11: CTMC cross sections for charge transfer in 10 keV Be^{2+} + H. The table includes the n, ℓ-distribution for $n \leq 5$, the n-distribution for $n \leq 10$, and the total charge transfer cross section for capture to all states. Cross sections are given in cm^2.

n	ℓ	σ_{nl}	σ_n	σ
1	0			
2	0	1.05e-16	5.76e-16	
2	1	4.69e-16		
3	0	1.85e-17	1.11e-16	
3	1	4.16e-17		
3	2	5.04e-17		
4	0	4.93e-18	2.72e-17	
4	1	8.62e-18		
4	2	6.55e-18		
4	3	7.11e-18		
5	0	1.44e-18	1.04e-17	
5	1	3.41e-18		
5	2	2.24e-18		
5	3	1.95e-18		
5	4	1.40e-18		
6	Σ		5.06e-18	
7	Σ		2.82e-18	
8	Σ		1.85e-18	
9	Σ		1.23e-18	
10	Σ		7.68e-19	
Σ	Σ			7.40e-16

Table 12: CTMC cross sections for charge transfer in 20 keV Be^{2+} + H. The table includes the n, ℓ-distribution for $n \leq 5$, the n-distribution for $n \leq 10$, and the total charge transfer cross section for capture to all states. Cross sections are given in cm^2.

n	ℓ	σ_{nl}	σ_n	σ
1	0			
2	0	2.80e-17	1.99e-16	
2	1	1.71e-16		
3	0	1.15e-17	8.76e-17	
3	1	5.65e-17		
3	2	1.96e-17		
4	0	6.39e-18	3.59e-17	
4	1	2.45e-17		
4	2	4.82e-18		
4	3	1.95e-19		
5	0	3.93e-18	1.73e-17	
5	1	1.14e-17		
5	2	1.78e-18		
5	3	1.92e-19		
5	4			
6	Σ		9.96e-18	
7	Σ		6.17e-18	
8	Σ		3.86e-18	
9	Σ		2.84e-18	
10	Σ		2.10e-18	
Σ	Σ			3.73e-16

Table 13: CTMC cross sections for charge transfer in 50 keV Be^{2+} + H. The table includes the n, ℓ-distribution for $n \leq 5$, the n-distribution for $n \leq 10$, and the total charge transfer cross section for capture to all states. Cross sections are given in cm^2.

n	ℓ	σ_{nl}	σ_n	σ
1	0			
2	0	4.90e-18	2.87e-17	
2	1	2.38e-17		
3	0	2.38e-18	1.42e-17	
3	1	1.02e-17		
3	2	1.58e-18		
4	0	1.33e-18	7.01e-18	
4	1	5.21e-18		
4	2	4.73e-19		
4	3			
5	0	7.73e-19	3.65e-18	
5	1	2.72e-18		
5	2	1.59e-19		
5	3			
5	4			
6	Σ		2.29e-18	
7	Σ		1.39e-18	
8	Σ		8.62e-19	
9	Σ		6.67e-19	
10	Σ		4.83e-19	
Σ	Σ			6.16e-17

Table 14: CTMC cross sections for charge transfer in 100 keV Be^{2+} + H. The table includes the n, ℓ-distribution for $n \leq 5$, the n-distribution for $n \leq 10$, and the total charge transfer cross section for capture to all states. Cross sections are given in cm^2.

n	ℓ	σ_{nl}	σ_n	σ
1	0			
2	0	4.80e-19	2.08e-18	
2	1	1.60e-18		
3	0	1.83e-19	7.83e-19	
3	1	5.89e-19		
3	2	1.13e-20		
4	0	9.04e-20	3.78e-19	
4	1	2.85e-19		
4	2	2.33e-21		
4	3			
5	0	5.97e-20	2.11e-19	
5	1	1.51e-19		
5	2	3.88e-22		
5	3			
5	4			
6	Σ		1.17e-19	
7	Σ		7.84e-20	
8	Σ		5.08e-20	
9	Σ		3.53e-20	
10	Σ		3.07e-20	
Σ	Σ			3.89e-18

Table 15: CTMC cross sections for charge transfer in 200 keV Be^{2+} + H. The table includes the n, ℓ-distribution for $n \leq 5$, the n-distribution for $n \leq 10$, and the total charge transfer cross section for capture to all states. Cross sections are given in cm^2.

n	ℓ	σ_{nl}	σ_n	σ
1	0	3.79e-16	3.79e-16	
2	0	6.19e-17	7.61e-16	
2	1	6.99e-16		
3	0	5.60e-17	1.23e-15	
3	1	2.57e-16		
3	2	9.16e-16		
4	0	1.15e-17	1.16e-16	
4	1	2.96e-17		
4	2	4.17e-17		
4	3	3.28e-17		
5	0	2.22e-18	1.60e-17	
5	1	4.92e-18		
5	2	4.95e-18		
5	3	2.84e-18		
5	4	1.03e-18		
6	Σ		4.63e-18	
7	Σ		2.13e-18	
8	Σ		1.10e-18	
9	Σ		6.67e-19	
10	Σ		4.73e-19	
Σ	Σ			2.51e-15

Table 16: CTMC cross sections for charge transfer ($\sigma_{q,q-1}$, sum of single charge transfer and transfer ionization) in 10 keV Be^{4+} + H_2. The table includes the n, ℓ-distribution for $n \leq 5$, the n-distribution for $n \leq 10$, and the total charge transfer cross section for capture to all states. Cross sections are given in cm^2.

n	ℓ	σ_{nl}	σ_n	σ
1	0	3.60e-16	3.60e-16	
2	0	4.22e-17	6.96e-16	
2	1	6.54e-16		
3	0	2.30e-17	9.77e-16	
3	1	1.65e-16		
3	2	7.89e-16		
4	0	9.27e-18	1.79e-16	
4	1	3.38e-17		
4	2	7.04e-17		
4	3	6.58e-17		
5	0	3.43e-18	3.56e-17	
5	1	1.07e-17		
5	2	1.33e-17		
5	3	6.81e-18		
5	4	1.34e-18		
6	Σ		1.20e-17	
7	Σ		6.03e-18	
8	Σ		3.25e-18	
9	Σ		2.03e-18	
10	Σ		1.39e-18	
Σ	Σ			2.28e-15

Table 17: CTMC cross sections for charge transfer ($\sigma_{q,q-1}$, sum of single charge transfer and transfer ionization) in 20 keV Be^{4+} + H_2. The table includes the n, ℓ-distribution for $n \leq 5$, the n-distribution for $n \leq 10$, and the total charge transfer cross section for capture to all states. Cross sections are given in cm^2.

n	ℓ	σ_{nl}	σ_n	σ
1	0	2.34e-16	2.34e-16	
2	0	2.25e-17	3.79e-16	
2	1	3.56e-16		
3	0	1.06e-17	4.67e-16	
3	1	8.40e-17		
3	2	3.72e-16		
4	0	6.43e-18	2.96e-16	
4	1	4.05e-17		
4	2	1.15e-16		
4	3	1.34e-16		
5	0	3.77e-18	1.27e-16	
5	1	2.13e-17		
5	2	5.13e-17		
5	3	4.86e-17		
5	4	2.47e-18		
6	Σ		6.27e-17	
7	Σ		3.50e-17	
8	Σ		2.08e-17	
9	Σ		1.42e-17	
10	Σ		9.93e-18	
Σ	Σ			1.69e-15

Table 18: CTMC cross sections for charge transfer ($\sigma_{q,q-1}$, sum of single charge transfer and transfer ionization) in 50 keV Be^{4+} + H_2. The table includes the n, ℓ-distribution for $n \leq 5$, the n-distribution for $n \leq 10$, and the total charge transfer cross section for capture to all states. Cross sections are given in cm^2.

n	ℓ	σ_{nl}	σ_n	σ
1	0	5.07e-17	5.07e-17	
2	0	1.16e-17	1.24e-16	
2	1	1.12e-16		
3	0	6.64e-18	1.58e-16	
3	1	4.11e-17		
3	2	1.10e-16		
4	0	3.97e-18	1.06e-16	
4	1	2.15e-17		
4	2	4.94e-17		
4	3	3.08e-17		
5	0	2.29e-18	6.34e-17	
5	1	1.27e-17		
5	2	2.71e-17		
5	3	2.10e-17		
5	4	2.66e-19		
6	Σ		4.03e-17	
7	Σ		2.72e-17	
8	Σ		1.85e-17	
9	Σ		1.28e-17	
10	Σ		9.71e-18	
Σ	Σ			6.56e-16

Table 19: CTMC cross sections for charge transfer ($\sigma_{q,q-1}$, sum of single charge transfer and transfer ionization) in 100 keV Be^{4+} + H_2. The table includes the n, ℓ-distribution for $n \leq 5$, the n-distribution for $n \leq 10$, and the total charge transfer cross section for capture to all states. Cross sections are given in cm^2.

n	ℓ	σ_{nl}	σ_n	σ
1	0	4.04e-18	4.04e-18	
2	0	3.32e-18	2.41e-17	
2	1	2.08e-17		
3	0	2.17e-18	2.36e-17	
3	1	9.29e-18		
3	2	1.21e-17		
4	0	1.22e-18	1.48e-17	
4	1	5.06e-18		
4	2	7.34e-18		
4	3	1.21e-18		
5	0	7.52e-19	8.73e-18	
5	1	2.92e-18		
5	2	4.07e-18		
5	3	9.80e-19		
5	4	.00e+00		
6	Σ		5.67e-18	
7	Σ		3.58e-18	
8	Σ		2.58e-18	
9	Σ		1.80e-18	
10	Σ		1.36e-18	
Σ	Σ			9.67e-17

Table 20: CTMC cross sections for charge transfer ($\sigma_{q,q-1}$, sum of single charge transfer and transfer ionization) in 200 keV Be^{4+} + H_2. The table includes the n, ℓ-distribution for $n \leq 5$, the n-distribution for $n \leq 10$, and the total charge transfer cross section for capture to all states. Cross sections are given in cm^2.

n	ℓ	σ_{nl}	σ_n	σ
1	0	5.53e-16	5.53e-16	
2	0	2.27e-16	8.44e-16	
2	1	6.17e-16		
3	0	4.54e-17	3.60e-16	
3	1	1.08e-16		
3	2	2.07e-16		
4	0	5.24e-18	2.72e-17	
4	1	9.65e-18		
4	2	8.48e-18		
4	3	3.85e-18		
5	0	1.21e-18	7.62e-18	
5	1	2.19e-18		
5	2	2.35e-18		
5	3	1.41e-18		
5	4	4.63e-19		
6	Σ		2.92e-18	
7	Σ		1.55e-18	
8	Σ		8.48e-19	
9	Σ		5.30e-19	
10	Σ		3.76e-19	
Σ	Σ			1.80e-15

Table 21: CTMC cross sections for charge transfer ($\sigma_{q,q-1}$, sum of single charge transfer and transfer ionization) in 10 keV Be^{3+} + H_2. The table includes the n, ℓ-distribution for $n \leq 5$, the n-distribution for $n \leq 10$, and the total charge transfer cross section for capture to all states. Cross sections are given in cm^2.

n	ℓ	σ_{nl}	σ_n	σ
1	0	4.75e-16	4.75e-16	
2	0	9.70e-17	6.64e-16	
2	1	5.67e-16		
3	0	2.62e-17	4.08e-16	
3	1	9.98e-17		
3	2	2.82e-16		
4	0	8.25e-18	5.28e-17	
4	1	2.04e-17		
4	2	1.69e-17		
4	3	7.22e-18		
5	0	2.76e-18	1.60e-17	
5	1	6.18e-18		
5	2	4.34e-18		
5	3	1.43e-18		
5	4	1.25e-18		
6	Σ		6.75e-18	
7	Σ		3.56e-18	
8	Σ		1.98e-18	
9	Σ		1.43e-18	
10	Σ		9.35e-19	
Σ	Σ			1.64e-15

Table 22: CTMC cross sections for charge transfer ($\sigma_{q,q-1}$, sum of single charge transfer and transfer ionization) in 20 keV Be^{3+} + H_2. The table includes the n, ℓ-distribution for $n \leq 5$, the n-distribution for $n \leq 10$, and the total charge transfer cross section for capture to all states. Cross sections are given in cm^2.

n	ℓ	σ_{nl}	σ_n	σ
1	0	2.15e-16	2.15e-16	
2	0	3.20e-17	3.33e-16	
2	1	3.01e-16		
3	0	1.27e-17	2.94e-16	
3	1	9.64e-17		
3	2	1.85e-16		
4	0	7.31e-18	1.22e-16	
4	1	4.70e-17		
4	2	6.13e-17		
4	3	6.15e-18		
5	0	4.47e-18	5.34e-17	
5	1	2.50e-17		
5	2	2.21e-17		
5	3	1.58e-18		
5	4	2.44e-20		
6	Σ		2.82e-17	
7	Σ		1.68e-17	
8	Σ		1.12e-17	
9	Σ		7.36e-18	
10	Σ		5.34e-18	
Σ	Σ			1.11e-15

Table 23: CTMC cross sections for charge transfer ($\sigma_{q,q-1}$, sum of single charge transfer and transfer ionization) in 50 keV Be^{3+} + H_2. The table includes the n, ℓ-distribution for $n \leq 5$, the n-distribution for $n \leq 10$, and the total charge transfer cross section for capture to all states. Cross sections are given in cm^2.

n	ℓ	σ_{nl}	σ_n	σ
1	0	3.60e-17	3.60e-17	
2	0	1.34e-17	1.12e-16	
2	1	9.84e-17		
3	0	6.61e-18	8.34e-17	
3	1	3.82e-17		
3	2	3.86e-17		
4	0	3.62e-18	4.52e-17	
4	1	2.04e-17		
4	2	2.03e-17		
4	3	9.21e-19		
5	0	2.11e-18	2.53e-17	
5	1	1.14e-17		
5	2	1.13e-17		
5	3	4.90e-19		
5	4			
6	Σ		1.51e-17	
7	Σ		1.00e-17	
8	Σ		6.55e-18	
9	Σ		4.67e-18	
10	Σ		3.52e-18	
Σ	Σ			3.57e-16

Table 24: CTMC cross sections for charge transfer ($\sigma_{q,q-1}$, sum of single charge transfer and transfer ionization) in 100 keV Be^{3+} + H_2. The table includes the n, ℓ-distribution for $n \leq 5$, the n-distribution for $n \leq 10$, and the total charge transfer cross section for capture to all states. Cross sections are given in cm^2.

n	ℓ	σ_{nl}	σ_n	σ
1	0	5.23e-18	5.23e-18	
2	0	3.12e-18	1.71e-17	
2	1	1.40e-17		
3	0	1.49e-18	1.02e-17	
3	1	6.25e-18		
3	2	2.44e-18		
4	0	8.53e-19	5.36e-18	
4	1	3.11e-18		
4	2	1.39e-18		
4	3	2.03e-21		
5	0	4.78e-19	2.92e-18	
5	1	1.70e-18		
5	2	7.42e-19		
5	3	2.03e-21		
5	4			
6	Σ		1.73e-18	
7	Σ		1.16e-18	
8	Σ		7.64e-19	
9	Σ		5.78e-19	
10	Σ		4.38e-19	
Σ	Σ			4.74e-17

Table 25: CTMC cross sections for charge transfer ($\sigma_{q,q-1}$, sum of single charge transfer and transfer ionization) in 200 keV Be^{3+} + H_2. The table includes the n, ℓ-distribution for $n \leq 5$, the n-distribution for $n \leq 10$, and the total charge transfer cross section for capture to all states. Cross sections are given in cm^2.

n	ℓ	σ_{nl}	σ_n	σ
1	0			
2	0	2.97e-16	9.68e-16	
2	1	6.71e-16		
3	0	1.42e-17	7.00e-17	
3	1	3.02e-17		
3	2	2.56e-17		
4	0	2.52e-18	1.61e-17	
4	1	5.64e-18		
4	2	4.94e-18		
4	3	3.04e-18		
5	0	8.97e-19	6.40e-18	
5	1	1.77e-18		
5	2	1.85e-18		
5	3	1.21e-18		
5	4	6.67e-19		
6	Σ		2.92e-18	
7	Σ		1.69e-18	
8	Σ		1.04e-18	
9	Σ		6.59e-19	
10	Σ		5.25e-19	
Σ	Σ			8.95e-16

Table 26: CTMC cross sections for charge transfer ($\sigma_{q,q-1}$, sum of single charge transfer and transfer ionization) in 10 keV Be^{2+} + H_2. The table includes the n, ℓ-distribution for $n \leq 5$, the n-distribution for $n \leq 10$, and the total charge transfer cross section for capture to all states. Cross sections are given in cm^2.

n	ℓ	σ_{nl}	σ_n	σ
1	0			
2	0	1.56e-16	8.05e-16	
2	1	6.49e-16		
3	0	2.25e-17	1.20e-16	
3	1	4.96e-17		
3	2	4.80e-17		
4	0	5.74e-18	3.12e-17	
4	1	1.20e-17		
4	2	6.98e-18		
4	3	6.48e-18		
5	0	2.21e-18	1.32e-17	
5	1	4.54e-18		
5	2	3.19e-18		
5	3	1.95e-18		
5	4	1.29e-18		
6	Σ		6.82e-18	
7	Σ		3.99e-18	
8	Σ		2.61e-18	
9	Σ		1.69e-18	
10	Σ		1.17e-18	
Σ	Σ			8.32e-16

Table 27: CTMC cross sections for charge transfer ($\sigma_{q,q-1}$, sum of single charge transfer and transfer ionization) in 20 keV Be^{2+} + H_2. The table includes the n, ℓ-distribution for $n \leq 5$, the n-distribution for $n \leq 10$, and the total charge transfer cross section for capture to all states. Cross sections are given in cm^2.

n	ℓ	σ_{nl}	σ_n	σ
1	0			
2	0	4.56e-17	3.30e-16	
2	1	2.84e-16		
3	0	1.67e-17	1.19e-16	
3	1	7.86e-17		
3	2	2.39e-17		
4	0	9.00e-18	4.79e-17	
4	1	3.30e-17		
4	2	5.52e-18		
4	3	3.77e-19		
5	0	5.76e-18	2.31e-17	
5	1	1.48e-17		
5	2	2.19e-18		
5	3	3.01e-19		
5	4			
6	Σ		1.31e-17	
7	Σ		7.82e-18	
8	Σ		5.12e-18	
9	Σ		3.44e-18	
10	Σ		2.69e-18	
Σ	Σ			5.05e-16

Table 28: CTMC cross sections for charge transfer ($\sigma_{q,q-1}$, sum of single charge transfer and transfer ionization) in 50 keV Be^{2+} + H_2. The table includes the n, ℓ-distribution for $n \leq 5$, the n-distribution for $n \leq 10$, and the total charge transfer cross section for capture to all states. Cross sections are given in cm^2.

n	ℓ	σ_{nl}	σ_n	σ
1	0			
2	0	1.15e-17	6.77e-17	
2	1	5.62e-17		
3	0	4.70e-18	2.66e-17	
3	1	1.96e-17		
3	2	2.30e-18		
4	0	2.34e-18	1.19e-17	
4	1	8.88e-18		
4	2	6.34e-19		
4	3			
5	0	1.36e-18	6.43e-18	
5	1	4.84e-18		
5	2	2.24e-19		
5	3	1.78e-21		
5	4			
6	Σ		3.74e-18	
7	Σ		2.42e-18	
8	Σ		1.62e-18	
9	Σ		1.09e-18	
10	Σ		8.50e-19	
Σ	Σ			1.21e-16

Table 29: CTMC cross sections for charge transfer ($\sigma_{q,q-1}$, sum of single charge transfer and transfer ionization) in 100 keV Be^{2+} + H_2. The table includes the n,ℓ-distribution for $n \leq 5$, the n-distribution for $n \leq 10$, and the total charge transfer cross section for capture to all states. Cross sections are given in cm^2.

n	ℓ	σ_{nl}	σ_n	σ
1	0			
2	0	1.56e-18	7.01e-18	
2	1	5.45e-18		
3	0	6.22e-19	2.59e-18	
3	1	1.93e-18		
3	2	3.93e-20		
4	0	2.72e-19	1.09e-18	
4	1	8.10e-19		
4	2	8.97e-21		
4	3			
5	0	1.70e-19	6.10e-19	
5	1	4.38e-19		
5	2	2.76e-21		
5	3			
5	4			
6	Σ		3.37e-19	
7	Σ		2.26e-19	
8	Σ		1.69e-19	
9	Σ		1.13e-19	
10	Σ		8.48e-20	
Σ	Σ			1.25e-17

Table 30: CTMC cross sections for charge transfer ($\sigma_{q,q-1}$, sum of single charge transfer and transfer ionization) in 200 keV Be^{2+} + H_2. The table includes the n, ℓ-distribution for $n \leq 5$, the n-distribution for $n \leq 10$, and the total charge transfer cross section for capture to all states. Cross sections are given in cm^2.